Vgll3 operates via Tead1, Tead3 and Tead4 to influence myogenesis in skeletal muscle

Nicolas Figeac[1,a)], Abdalla D. Mohamed[2,4,a)], Congshan Sun[1,3)], Martin Schönfelder[5)], David Matallanas[6)], Amaya Garcia-Munoz[6)], Edoardo Missiaglia[7)], Elaina Collie-Duguid[8)], Vanessa De Mello[2)], Ajaybabu V. Pobbati[9)], Johanna Pruller[1], Oihane Jaka[10)], Stephen D. R. Harridge[10)], Wanjin Hong[9)], Janet Shipley[11)], Neil Vargesson[2)], Peter S. Zammit[1,b)*] and Henning Wackerhage[2,5,b)*]

[1] King's College London, Randall Centre for Cell and Molecular Biophysics, London, SE1 1UL, UK.
[2] University of Aberdeen, School of Medicine, Medical Sciences and Nutrition, Foresterhill, Aberdeen, AB25 2ZD, Scotland.
[3] Department of Neurology, The Johns Hopkins School of Medicine, Baltimore, Maryland, USA
[4] Institute of Developmental Genetics, Helmholtz Zentrum München, German Research Center for Environment and Health, Ingolstaedter Landstrasse 1, D-85764 Munich / Neuherberg, Germany
[5] Technical University of Munich. Faculty of Sport and Health Sciences. Georg-Brauchle-Ring 60, 80992 Munich, Germany
[6] Systems Biology Ireland; Conway Institute; Belfield; Dublin 4; Ireland.
[7] Institute of Pathology, Lausanne University Hospital (CHUV), Lausanne, Switzerland
[8] University of Aberdeen, Centre for Genome Enabled Biology and Medicine, 23 St Machar Drive, Aberdeen, AB24 3RY, Scotland.
[9] Institute of Molecular and Cell Biology, A-STAR, 61 Biopolis Drive, Singapore 138673, Singapore
[10] Centre for Human and Applied Physiological Sciences, King's College London, London, UK.
[11] Sarcoma Molecular Pathology Team, Divisions of Molecular Pathology and Cancer Therapeutics, Institute of Cancer Research, London, UK

[a)] Joint first authors
[b)] Joint senior authors
* corresponding authors Zammit: peter.zammit@kcl.ac.uk and Wackerhage henning.wackerhage@tum.de

Key Words: Vgll3, Yap, Taz, Skeletal muscle, stem cells

Summary Statement

Vgll3 interacts with TEAD transcription factors to direct expression of crucial muscle regulatory genes and contribute to control of skeletal myogenesis.

JCS Advance Online Article. Posted on 28 May 2019

Abstract

VGLL proteins are transcriptional co-factors that bind TEAD family transcription factors to regulate events ranging from wing development in fly, to muscle fibre composition and immune function in mice. Here, we characterise *Vgll3* in skeletal muscle. *Vgll3* is expressed at low levels in healthy muscle but levels increase during hypertrophy or regeneration, and in disease, *VGLL3* is highly expressed in dystrophic muscle and alveolar rhabdomyosarcoma. Interaction proteomics revealed that VGLL3 binds TEAD1,3,4 in myoblasts and/or myotubes. However, there is no interaction with proteins of major regulatory systems such as the Hippo kinase cascade, unlike the TEAD co-factors YAP and TAZ. *Vgll3* overexpression reduces the Hippo negative feedback loop, affecting expression of muscle-regulating genes including *Myf5, Pitx2/3*, *Wnts* and *IGFBP*. Vgll3 mainly represses gene expression, regulating similar genes to that of *YAP1* and *TAZ*. SiRNA-mediated *Vgll3* knockdown suppresses myoblast proliferation, while *Vgll3* overexpression strongly promotes myogenic differentiation. Skeletal muscle is overtly normal in *Vgll3*-null mice though, presumably due to feedback signalling and/or redundancy. This work identifies Vgll3 as a transcriptional co-factor operating with the Hippo signal transduction network to control myogenesis.

Introduction

The Hippo signal transduction network regulates development, stem cell identity and function, cell proliferation, organ and body size (Hansen et al., 2015; Piccolo et al., 2014; Tremblay and Camargo, 2012). Hippo proteins also have major functions in skeletal muscle (Wackerhage et al., 2014). Here, especially the Hippo effector Yap (gene symbol *YAP1*) but also other proteins such as the Yap paralogue Taz (gene symbol *WWTR1*), vestigial-like factors (Vgll) 1-4 and the TEA domain (Tead) 1-4 transcription factors have been linked to both developmental and regenerative myogenesis (Chen et al., 2004; Gunther et al., 2004; Judson et al., 2012; Maeda et al., 2002; Mielcarek et al., 2002; Mielcarek et al., 2009; Sun et al., 2017; Watt et al., 2010). For example, both YAP and TAZ are expressed in muscle stem (satellite) cells, where they promote proliferation, and while TAZ enhances subsequent myogenic differentiation into multinucleated myotubes, YAP inhibits this process (Judson et al., 2012; Sun et al., 2017). This transcriptional network also plays a role in genetic muscle disease (Bertrand et al., 2014; Judson et al., 2013) and development of rhabdomyosarcomas – sarcomas with characteristics of skeletal muscle (Mohamed et al., 2016; Slemmons et al., 2015; Tremblay et al., 2014). Hippo/Vgll proteins also affect muscle fibre type distribution (Honda et al., 2017; Tsika et al., 2008), and can cause skeletal muscle hypertrophy (Goodman et al., 2015; Watt et al., 2015). Finally, Hippo proteins are candidate regulators of adaptation to exercise training (Gabriel et al., 2016).

The term “Hippo” stems from a kinase-encoding gene whose mutagenesis resulted in the puckered appearance of the head in fly, reminiscent of the skin of a Hippopotamus. At the centre of the Hippo signal transduction network are the transcriptional co-factors Yap and Taz that bind and co-activate Tead1-4 transcription factors to regulate gene expression. The Hippo pathway is a signalling cascade where the kinases Mst1 and Mst2 regulate Lats1 and Lats2 by phosphorylation. In turn Lats1 and Lats2 inhibit Yap/Taz dependent gene regulation through inhibitory phosphorylation of multiple serine residues, which prevent nuclear translocation and so interaction with Tead1-4 (Hansen et al., 2015). However, Yap/Taz-Tead1-4 are not only regulated by the Hippo pathway, but also by many other signalling systems including AMPK, mechanotransduction, G protein-coupled receptors, and Wnt signalling that communicate with the Hippo pathway (Hansen et al., 2015). This is why the term “Hippo signal transduction network” arguably best describes the overall signalling system whose main molecular function is transcriptional regulation through Tead1-4 transcription factors.

The *Vgll1-4* genes are homologous to the *vestigial* gene in fly and also bind Tead family transcription factors, so Vglls can operate in a similar manner as Yap and Taz to organise transcription. Vestigial and Vgll proteins use their Tondu domain (Vaudin et al., 1999) to bind via two interfaces, the same Tead site also bound by Yap via three interfaces (Pobbati et al., 2012). Loss of *vestigial* reduces the wings of flies to vestiges (reviewed in (Simon et al., 2016)), which

requires the Tead homologue *scalloped* (Halder et al., 1998). In mammals, *Vgll1-3* have one Tondu domain, and are expressed in a tissue-specific fashion, while *Vgll4* has two Tondu domains and is ubiquitously expressed. Functionally, Vgll4 is a Yap-Tead repressor or antagonist, whereas Vgll1-3 have been suggested to be "selector" genes that specify cell and tissue types (Koontz et al., 2013). Recently, Ets1 was identified as an additional Vgll3-binding transcription factor, suggesting that Teads are not the only transcription factors that are co-regulated by Vglls (Simon et al., 2017). If transcriptional regulation through Tead1-4 is the output of Hippo-related signalling, then this suggests that Vgll1-4 integrate into the wider Hippo signal transduction network.

Vglls have been linked to skeletal muscle. Fly *vestigial* has been implicated in flight muscle development (Bernard et al., 2009). In mammals, *Vgll2* (*Vito-1*) and *Vgll3* (*Vito-2*) have been studied in relation to skeletal muscle, especially by the Braun and Stewart groups (Chen et al., 2004; Gunther et al., 2004; Maeda et al., 2002; Mielcarek et al., 2002; Mielcarek et al., 2009). *Vgll2* has an important role in adult muscle *in vivo,* as *Vgll2*$^{-/-}$ mice have a higher number of fast-twitch type IIb muscle fibres and down-regulation of the *Myh7* slow type I gene (Honda et al., 2017). *Vgll3*$^{-/-}$ mice have a sex-linked immune phenotype (Liang et al., 2017) and a shortened QT interval (http://www.mousephenotype.org/data/genes/MGI:1920819) but it is unknown whether knockout of *Vgll3* affects myogenesis or adult skeletal muscle. Copy number alterations of *VGLL3* and *YAP1* have been reported for human soft tissue sarcomas including rhabdomoysarcomas where VGLL3 is required for proliferation (Cancer Genome Atlas Research Network. Electronic address and Cancer Genome Atlas Research, 2017; Helias-Rodzewicz et al., 2010).

Here, we analyse the regulation and molecular/cellular function of Vgll3 in skeletal muscle *in vitro* and *in vivo,* with reference to the roles of YAP and TAZ. *Vgll3* is expressed at low levels in healthy muscle but expression increases both during muscle hypertrophy and muscle regeneration. In disease settings, *VGLL3* is also highly expressed in dystrophic muscle and alveolar rhabdomyosarcoma. *Vgll3* expression increases as human and murine myoblasts undergo myogenic differentiation ex-vivo. *VGLL3* knockdown suppresses myoblast proliferation, while constitutive *VGLL3* expression enhances myogenic differentiation. However, adult skeletal muscle fibre types and structure are unaffected in *Vgll3*-null mice, presumably due to redundancy and/or feedback signalling. Proteomics revealed that VGLL3 binds transcription factors TEAD1, TEAD3 AND TEAD4 in myoblasts and/or myotubes, but no interactions were detected with major regulatory systems such as kinases. Transcriptomic analysis shows that Vgll3 regulates the Hippo negative feedback loop, and affects expression of genes controlling myogenesis including *Myf5, Pitx2/3*, *Wnts* and *IGF-binding proteins*. Thus we conclude that Vgll3 is a transcriptional co-factor that operates in parallel with the Hippo effectors Yap and Taz to control myoblast proliferation and differentiation.

Results

Vgll2 and Vgll3 expression in skeletal muscle and cancer

The Hippo effector Yap, as well as Vgll1 and Vgll4, are able to bind Tead family transcription factors (Koontz et al., 2013; Pobbati et al., 2012). However, whilst Yap is regulated by a plethora of signalling mechanisms including phosphorylation, methylation, ubiquitination, sumoylation and localization changes, far less is known about regulation of Vglls. We therefore investigated regulation of Vgll3 and Vgll2, a paralogue that is highly expressed in skeletal muscle. While *VGLL2* is clearly expressed at higher levels in human muscle, VGLL3 is not (**Figure 1a and b**). To examine whether Vgll3 and Vgll2 are regulated transcriptionally, we analysed published datasets from GEO (see also supplementary Figure **S1**) and supplementary datafiles from published papers. This revealed that *VGLL3* expression is >3-fold higher in the quadriceps of boys with Duchenne muscular dystrophy compared to healthy quadriceps (**Figure 1c,** *VGLL2* is similar Supplementary Data **S1A** (Haslett et al., 2003). In mice, mean *Vgll3* expression increases both in synergist ablation-loaded, hypertrophying plantaris muscle (Chaillou et al., 2013) or in cardiotoxin-induced regenerating tibialis anterior muscle (Lukjanenko et al., 2013) (**Figure 1e and f)**. In contrast, *Vgll2* declines in both situations (Supplementary Figure **S1**).

An earlier study reported that the *PAX3-FOXO1* fusion gene induced *Vgll3* by 8-fold in the forelimb buds of mouse embryos at E10.5 (Lagha et al., 2010). Given that alveolar rhabdomyosarcomas (ARMS) frequently carry *PAX3-FOXO1* or *PAX7-FOXO1* fusion genes, we also analysed *VGLL3* expression in ARMS (Missiaglia et al., 2012; Shern et al., 2014). This showed that average *VGLL3* expression is highest in *PAX3-FOXO1* alveolar rhabdomyosarcomas when compared to other forms of rhabdomyosarcoma, myoblasts or differentiated muscle (**Figure 1d**). Finally, *Vgll3* expression is 2.3-fold higher in mouse embryonal rhabdomyosarcomas caused by YAP1 S127A expression in activated satellite cells, than in control skeletal muscle (Tremblay et al., 2014). In mouse muscle, a VGLL2 serine 261 phosphopeptide is detectable, but no VGLL3 phosphopeptides (Potts et al., 2017). This is relevant since fly vestigial is phosphorylated at Ser215 by p38 kinase (Pimmett et al., 2017). In human muscle, neither VGLL2 nor VGLL3 phosphopeptides are detectable pre- or post-intensive exercise (Hoffman et al., 2015). Together, this suggests that Vgll3 and Vgll2 are mainly regulated through their protein levels via transcription, rather than post-translation modifications.

VGLL3 binding protein partners in murine myoblasts and myotubes

In fly, vestigial protein binds the transcription factor scalloped (the orthoparalogue of mammalian Tead1-4) to create “wing cell-specific DNA-binding selectivity” for scalloped (Halder and Carroll, 2001; Halder et al., 1998). VGLL proteins also interact with the TEAD family of transcription factors, where the core complex structure of VGLL1 and TEAD4 reveals that the TONDU domain in VGLL1

interacts with TEAD4 by forming two interfaces (Pobbati et al., 2012). Subsequently, VGLL4 was also shown to pair with TEAD by forming similar interfaces (Jiao et al., 2014). The Tondu domains in *Drosophila* Vestigial and VGLL proteins are highly conserved. Thus, the core complex structure of VGLL3 with TEAD should be similar to that of VGLL1 or VGLL4. To test our prediction, we modelled the VGLL3-TEAD4 structure using the PHYRE2 protein fold recognition server. Superposition of VGLL1-TEAD4 and VGLL4-TEAD4 crystal structures with the modelled VGLL3-TEAD4 structure shows that all three binary core complexes are structurally similar (**Figure 2a**). To test whether VGLL3 and TEAD interact experimentally, we overexpressed HA-TEAD2 with Myc-VGLL3 and known interactor YAP, in HEK293 cells and then immunoprecipitated HA-TEAD2, Myc-VGLL3 or YAP (**Figure 2b)**. This demonstrated that VGLL3 binds TEAD2, and that Myc-VGLL3 reduces binding of YAP to TEAD2, suggesting that Myc-VGLL3 and YAP compete to bind HA-TEAD2. Using a fluorescently labelled YAP and TEAD4, we also verified that VGLL3 directly competes with YAP (**Figure 2c**). Addition of TEAD4 to labelled YAP results in the formation of YAP-TEAD4 complex that could be monitored in a native gel. Introduction of TONDU domain-containing VGLL3 peptide reduces the amount of YAP-TEAD4 complex in a dose-dependent manner (**Figure 2c**), suggesting a direct competition between YAP and VGLL3 for binding to TEAD4.

To systematically characterise VGLL3-binding proteins in muscle in a non-biased fashion, we over-expressed and co-immunoprecipitated VGLL3-flag from murine C2C12 myoblasts and myotubes and identified VGLL3-binding proteins through liquid chromatography and mass spectrometry (LC-MS). Identification of the bait VGLL3-flag (**Figure 2d**) shows that immunoprecipitation worked. In addition, identification of TEAD1 (**Figure 2e**), TEAD3 (**Figure 2f**) and TEAD4 (**Figure 2g**) confirms that VGLL3 can bind TEAD family transcription factors in myoblasts and myotubes. Binding to TEAD isoforms was different depending on the state of myogenic differentiation. VGLL3-TEAD1 and VGLL3-TEAD3 interaction do not change overtly between myoblasts and myotubes. Interaction between VGLL3 with TEAD4 however, was greater in myotubes, indicating that this complex likely has a role in the regulation of differentiation. Importantly, we did not identify other transcription factors among the co-immunoprecipitated proteins.

VGLL3 interaction proteomics also identified other proteins that interact with VGLL3 or through which VGLL3 additionally exerts its function. VGLL3 bound only 8 proteins in C2C12 myoblasts, but 52 proteins in C2C12 myotubes. In addition to TEAD1, 3, 4 (**Figure 2e-g),** VGLL3 also binds these classes of proteins in myoblasts and/or myotubes (full protein list - Supplemental Table **S1**):

a) Heat shock and related proteins (HSP90AA1, HSPA1L, HSPA8, HSPA9, HSPB1, HSPH1, CRYAB, DNAJA1, DNAJA2, DNAJB11).
b) Tubulins (TUBA1A, TUBB2A, TUBB4B, TUBB6).
c) Metabolic enzymes/proteins (AK1, AKR1B1, GAPDH, HADHB).

d) Mitochondrial channel proteins (VDAC1, VDAC2, SLC25A11, SLC25A5, TIMM50).
e) Ras-related proteins (RAB10, RAB5A AND RALA).

It should be noted however, that heat shock proteins, tubulins and metabolic proteins such as GAPDH are frequently detected in proteomic studies (Wang et al., 2009) and may be proteins generally linked to the synthesis and folding of proteins.

We illustrate the functional interaction between VGLL3-binding proteins for C2C12 myoblasts (**Figure 2h**) and C2C12 myotubes (**Figure 2i)**. The clear difference in the VGLL3 interactome in myoblast versus myotubes suggests that the role VGLL3 in myogenic differentiation is at least partially regulated by changes in protein-protein interactions. Most prominent is the differential interaction with the TEAD isoforms, with VGLL3 interaction with TEAD1 and TEAD3 in myoblasts, but TEAD1, TEAD3 and, importantly, TEAD4 in myotubes. This is consistent with our previous observations that *Tead4* mRNA, and TEAD1 and TEAD4 protein increase markedly during myogenic differentiation (Sun et al., 2017). Changes in Vgll3-mediated transcription are thus likely related to this differential availability of TEAD isoforms. Overall, there was only minimal overlap with YAP and TAZ-binding proteins with the exception of TEAD1, TEAD3 and TEAD4 (Supplemental Table **S2** and (Sun et al., 2017)). Moreover, most putative binding partners of VGLL3 normally reside in the cytosol. Whilst many of these proteins are associated with the synthesis of VGLL3, it might also suggest that VGLL3 can localise to both the nucleus and cytosol. We used the nuclear export signal-prediction programme NetNes 1.1. to search for a nuclear export signal in the human VGLL3 amino acid sequence. This revealed a “MQDSLEVTL” (single amino acid code) nuclear export signal that was fully conserved between man, chimpanzee, cat and mouse (Supplemental Table **S3**).

Transcriptomic analysis of VGLL3 target gene expression

Given that VGLL3 binds the same TEAD1, TEAD3 and TEAD4 transcription factors that are also bound by YAP and TAZ (Sun et al., 2017), we next assessed the effect of VGLL3 on gene expression in murine primary satellite cell-derived myoblasts. We compared the effects of VGLL3 on gene expression to our previous transcriptomic examination using YAP1 S127A or TAZ S89A (Sun et al., 2017). YAP1 S127A/TAZ S89A mutants are constitutively active because a serine residue is mutated to an alanine so that YAP or TAZ can no longer be inhibited by Ser127 or Ser89 phosphorylation respectively, which normally prevents nuclear localisation. Using a cutoff difference of ≥30% or ≤30% and false discovery rate (FDR) <10%, we found that VGLL3 only induced 1 gene and down-regulated 9 genes in myoblasts after 24 h. However, VGLL3 enhanced 29 genes and lowered expression of 126 genes after 48 h (**Figure 3a,** full list of VGLL3-regulated genes in Supplemental Table **S4**). Since, VGLL3 represses 5.2 times as many genes than it

induces, this identifies VGLL3 as a protein that mainly represses its target genes expression in myoblasts.

As predicted, many of the VGLL3-regulated genes are also regulated by YAP1 S127A and TAZ S89A ((Sun et al., 2017), listed in Supplemental Table **S5**). To illustrate this, we plotted all genes whose expression was significantly (FDR <10%) up-regulated (by ≥30%) or down-regulated (by ≤30%) in response to VGLL3 over expression. Many of the genes down-regulated by VGLL3 are up-regulated by YAP S127A and vice versa, suggesting an antagonistic effect (**Figure 3b** and Supplemental Table **S5**). There are however, genes that are down-regulated by both YAP1 S127A and VGLL3 (**Figure 3b**, lower left). Interestingly, VGLL3 or YAP1 S127A never induced the same gene (**Figure 3b**). In contrast, VGLL3 and TAZ S89A could both induce the same genes, but again, there was no clear agonist-antagonist relationship (**Figure 3c** and Supplemental Table **S5**).

VGLL3 negatively regulates (≥1.3 fold and FDR <10%) many crucial genes of the Hippo signal transduction network including the Hippo transcriptional co-factors *Wwtr1* (encoding Taz: down by 1.4-fold) and *Vgll2* (down by 2.1-fold), in addition to also suppressing *Ajuba, Amotl2* and *Frmd6* (down 1.5 - 1.8 fold) (**Figure 3a** and Supplementary Tables **S4** and **S5**). As TAZ S89A drives expression of *Vgll2* and *Vgll3* (Sun et al., 2017), this suggests that VGLL3, TAZ and VGLL2 cross-regulate each other. Other down-regulated genes include *Fzd4F,* the myokine *Flst1*, the paired-like homeodomain transcription factors *Pitx2* and *Pitx3,* and the IGF binding proteins *Igfbp2* and *Igfbp4.* By contrast, VGLL3 promotes expression of the myogenic regulatory factor *Myf5,* the growth factor receptor *Egfr*, the Wnt pathway member *Wnt7b* and the IGF binding protein *Igfbp3* (**Figure 3a** and Supplementary Tables **S4** and **S5**).

Genes identified as down-regulated by VGLL3 overexpression from our transcriptomic studies in mouse (**Figure 3**) were also analyzed in human myoblasts and myocytes after VGLL3 knockdown or over-expression (Supplemental Table **S6).** Most genes deregulated by VGLL3 overexpression in mouse were validated in man: with down-regulation of *VGLL2, AJUBA, AMOTL2, FSTL1* and *FZD4*, with *EGFR1* also repressed, while *WWTR1* was induced, and *FRMD6* and *PITX2/3* unchanged (Supplementary Table **S6)**.

Vgll3 expression dynamics and localisation during myogenesis

To study expression of *Vgll2* and *Vgll3* in mouse satellite cells and human primary myoblasts during myogenic progression, we first used RT-qPCR. Generally *Vgll2* and *Vgll3* expression increased during myogenic differentiation, with *Vgll3* increased in both mouse and human differentiating myoblasts, while *Vgll2* only increased transiently in mouse (**Figure 4a** and **b**). In man, *VGLL2* is selectively expressed in skeletal muscle, whereas *VGLL3* expression is low in muscle compared to other tissues (**Figure 1a and b**). To analyse protein distribution, we

purchased commercially available anti-VGLL3 antibodies, but found immunolabeling unchanged upon retroviral-mediated constitutive VGLL3 expression (data not shown). Instead, we designed a retroviral vector encoding *Flag-Vgll3* and used anti-Flag antibodies to detect the Flag-tagged VGLL3 protein. This showed that VGLL3 was located in the nucleus and cytoplasm of C2C12 murine myoblasts (**Figure 4c** and **d**). Upon myogenic differentiation into myocytes and multi-nucleated myotubes however, there was clear and robust nuclear localisation of Flag-tagged VGLL3 (**Figure 4e** and **f**).

Vgll3 supports proliferation and differentiation in mouse and human myoblasts

To assess Vgll3 function in myoblasts, we first employed siRNA-mediated down-regulation of Vgll3, which significantly reduced proliferation of both primary murine satellite cell-derived myoblasts and the human C25Cl48 immortalised myoblast line (Mamchaoui et al., 2011) (**Figure 5a** and **b**). This was particularly striking in human myoblasts, where EDU incorporation after a 2 hour EDU pulse dropped from 49.2% to 0.3% when VGLL3 was knocked-down (**Figure 5b**), suggesting that VGLL3 is essential for proliferation of human myoblasts. We next evaluated the impact of VGLL3 knock-down on myogenic differentiation to form multinucleated myotubes and assemble sarcomeres. VGLL3 down-regulation reduced murine myotube formation, as indicated by a drop in the proportion of nuclei within myotubes (fusion index) from 68.8% to 40.7% (**Figure 5c**) and in human myoblasts from 68.8% to 11.2% (**Figure 5d**). Especially in human myoblasts though, the reduced differentiation measured in VGLL3 down-regulated cells may be largely indirect, being at least partially explained by the presence of fewer myoblasts due to their reduced proliferation rate, even though siRNA-transfected cells were replated at the same density as controls before inducing differentiation.

We then examined retroviral-mediated overexpression of VGLL3 on proliferation and differentiation in transiently transduced primary murine satellite cell-derived myoblasts and stable *VGLL3*-expressing human C25Cl48 immortalised myoblasts. Vgll3 overexpression did not further increase mouse satellite cell proliferation (**Figure 5e**) but in human myoblasts, the proportion of EDU positive myoblasts dropped slightly to 26.0%, from 32.8% in myoblasts transduced with control retrovirus (**Figure 5f**). VGLL3 overexpression increased the fusion index in mouse satellite cell-derived myoblasts to 80.4%, from 43.2% with the control (**Figure 5g**) and to 61.0% from 35.4% in human myoblasts (**Figure 5h**). Together, these results in mouse and human myoblasts show that *Vgll3* expression enhances myoblast differentiation.

Vgll3-null mice have normal skeletal muscle and myoblast function

To examine the role of *Vgll3* in skeletal muscle development and maintenance *in vivo*, we characterised skeletal muscle of hind limbs of *Vgll3*$^{-/-}$ mice, generated as part of the International Phenotyping Consortium (Brown and Moore, 2012). *Vgll3*$^{-/-}$ mice were viable, born in the expected

Mendelian ratios and did not show any overt phenotype while reaching adulthood. The extensor digitorum longus (EDL) and soleus muscles of adult *Vgll3*$^{-/-}$ mice and wildtype controls were analysed independently by the London (**Figure 6**) and Munich (Supplementary Figure **S2** and Table **S7**) teams. We found no significant difference between the EDL and Soleus of *Vgll3*$^{-/-}$ and wildtype control mice in fibre type distribution (**Figure 6a and d**), satellite cells per muscle fibre (**Figure 6b**), and fibre numbers and size (**Figure 6c and e**). This shows that the constitutive loss of Vgll3 function can be compensated for *in vivo*, suggesting that Vgll3 is not essential for normal skeletal muscle development. Interestingly, satellite cell-derived myoblasts isolated from *Vgll3*$^{-/-}$ mice did not show any changes in proliferation rate compared to wildtype controls, as determined by measuring EdU incorporation following a 2 h pulse (**Figure 7a** and **b**). Expression of *Pax7, Myogenin, Vgll2 and Vgll4* were also unchanged in *Vgll3*$^{-/-}$ mice compared to wildtype controls (Supplementary Figure **S3**). Finally, differentiation of *Vgll3*$^{-/-}$ satellite cell-derived myoblasts was assessed by calculating the fusion index to test their ability to form multinucleated myotubes and area occupied by MyHC-expressing myotubes, but again no statistically significant differences were found compared to wildtype controls (**Figure 7c** and **d**)**.**

Discussion

Here we report a comprehensive analysis of the regulation, protein binding and effect on target gene expression of the transcriptional co-regulator Vgll3 in skeletal muscle, and compare Vgll3 with Yap and Taz. Additionally, we characterise Vgll3 function in skeletal muscle in vitro and in vivo.

Whilst *Vgll2* is highly expressed in skeletal muscle and involved in myogenic differentiation (Chen et al., 2004) and muscle fibre type distribution (Honda et al., 2017), far less is known about regulation and function of Vgll3 in adult skeletal muscle. Generally, *Vgll3* is expressed at low levels in healthy muscle, but levels increase during regeneration (Lukjanenko et al., 2013) and in mechanically loaded, hypertrophying plantaris muscle (Chaillou et al., 2013). *VGLL3* is also differentially expressed in human muscle-related disease, with a >3-fold increase in quadriceps muscles of Duchenne muscular dystrophy patients (Haslett et al., 2003). Copy number gains of the *VGLL3* gene have also been reported for some rhabdomyosarcomas (Helias-Rodzewicz et al., 2010) and in sarcomas (Cancer Genome Atlas Research Network. Electronic address and Cancer Genome Atlas Research, 2017; Helias-Rodzewicz et al., 2010). Moreover, *VGLL3* expression is high in alveolar rhabdomyosarcoma (ARMS) associated with *PAX3-FOXO1* and *PAX7-FOXO1* fusion genes (Missiaglia et al., 2012; Shern et al., 2014) when compared to other cancers and controls. High expression of VGLL3 in *PAX3-FOXO1* fusion gene-positive ARMS is intriguing because expression of the *PAX3-FOXO1* fusion gene in mouse embryos induces *Vgll3* expression in the forelimb bud at E10.5 by 8-fold (Lagha et al., 2010; Missiaglia et al., 2012; Shern et al.,

2014). Furthermore, a ChIP-Seq analysis of *PAX3-FOXO1* target genes reported *VGLL3* as a direct *PAX3-FOXO1* target (Cao et al., 2010). Collectively, this suggests that VGLL3 is controlled at the transcriptional level when myoblasts proliferate or muscle hypertrophies. This contrasts with the Hippo effectors YAP and TAZ, which are regulated by an extensive Hippo signal transduction network that regulates via protein modification (phosphorylation).

In fly, *vestigial* binds the Tead homologue *scalloped* (Halder and Carroll, 2001; Halder et al., 1998). VGLLs and TEADs also interact in mammals (Koontz et al., 2013; Pobbati et al., 2012) but recently ETS1 has been identified as a non-TEAD transcription factor that can be bound by VGLL3 (Simon et al., 2017). Our proteomic analysis of VGLL3-flag binding proteins in C2C12 myoblasts and myotubes revealed that VGLL3 competes for the same TEAD1, TEAD3 and TEAD4 transcription factors as bound by YAP and TAZ in these cells (Sun et al., 2017). The clear difference in the VGLL3 interactome in myoblast versus myotubes however, indicates that the role of this protein in myogenic differentiation is in part, regulated by changes in protein-protein interaction. This includes differential interaction with the TEAD isoforms, with interaction with TEAD1 and TEAD3 in myoblasts, but TEAD1, TEAD3 and TEAD4 in myotubes. This is consistent with previous observations on the expression dynamics of *Tead1-4* mRNA, and TEAD1 and TEAD4 protein, where TEAD4 levels increase markedly during myogenic differentiation (Benhaddou et al., 2012; Sun et al., 2017). Indeed, Tead4 knockdown inhibits myogenic differentiation in satellite cell-derived myoblasts (Sun et al., 2017). Changes in VGLL3-mediated transcription between myoblasts and myotubes are thus likely related to this differential availability of the TEAD isoforms for activation by VGLL3.

TEAD1, TEAD3 and TEAD4 are the only proteins that are co-immunoprecipitated together with VGLL3, YAP and TAZ. Whilst YAP and TAZ share 18.6% of their binding partners, VGLL3 only shares ~1% of the binding partners with YAP or TAZ, respectively. Moreover, we could only identify the phosphatase PPP2R1A as a potential, protein-modifying regulator among the VGLL3-binding proteins. Interestingly, PPP2R1A is functionally relevant in ARMS (Akaike et al., 2018), where VGLL3 is highly expressed. With VGLL3, we additionally co-immunoprecipitated many cytosolic proteins including proteins involved with protein processing in the endoplasmic reticulum, especially heat shock proteins, and components of the tubulin cytoskeleton. Localisation of VGLL3 using a Flag-tagged version revealed VGLL3 in both the nucleus and cytoplasm in myoblasts, so VGLL3 interaction with cytoplasmic proteins is likely. We also discovered the presence of a nuclear export signal in VGLL3. However, heat shock proteins, tubulins and metabolic proteins such as GAPDH are frequently detected in proteomic studies (Wang et al., 2009) and may be generally linked to the synthesis and folding of proteins such as Flag-VGLL3, although others might be false positives such as flag-binding proteins.

Given that VGLL3, YAP and TAZ compete for the same TEAD1,3,4 transcription factors (Sun et al., 2017), do VGLL3, YAP and TAZ regulate the same genes as agonists or antagonists? We compared our new VGLL3 transcriptomic analysis in myoblasts to our earlier data, where we measured the effect of YAP1 S127A and TAZ S89A on gene expression (Sun et al., 2017). This revealed that ~5 times more genes were down-regulated by VGLL3, than induced, suggesting that VGLL3 acts mainly to reduce its target gene expression. In the VGLL3 interactome data however, we found no obvious binding partner with a known repressor function. In contrast to VGLL3, YAP induces and represses similar numbers of genes (Judson et al., 2012; Sun et al., 2017). While there was a broad overlap between genes regulated by VGLL3, YAP1 S127A and TAZ S89A, there is no simple agonist or antagonist relationship. For example, VGLL3, YAP1 S127A and TAZ S89A all repress genes such as *Igfbp4*. In contrast, the Hippo gene *Amotl2* is down-regulated by VGLL3 and induced by TAZ S89A and YAP1 S127A, suggesting that VGLL3 and YAP/TAZ act as antagonists in relation to *Amotl2* expression. Most genes deregulated by VGLL3 overexpression in mouse were also similarly affected by VGLL3-overexpression in human myoblasts.

When analysing individual genes, some genes groups and individual genes stood out. First, VGLL3 mainly down-regulated the YAP-induced Hippo genes *Ajuba, Amotl2, Frmd6* that are induced by YAP1 S127A, and which we have previously termed the Hippo negative feedback loop (Judson et al., 2012). Additionally, VGLL3 repressed *Vgll2* in man and mouse, and also repressed the Hippo transcriptional co-factors *Wwtr1* (encoding Taz) in mouse, but enhanced *WWTR* in man. Differences in effects of VGLL3 on gene expression between mouse and man can possibly be explained by complexity of the Tead-transcriptional system. There are 4 Tead transcription factors, Yap, Taz and 4 Vglls. These factors play a crucial role during myogenic progression (Sun et al., 2017; Watt et al., 2010) and change expression during differentiation ((Sun et al., 2017) and this study). Such complex regulation also involves negative feedback loops regulated by Yap/Taz and Tead1-4 (Judson et al., 2012). Thus, depending on protein levels, the state of differentiation, and activity of the negative feedback loop, expression of target genes can vary between species.

In addition to the Hippo-related genes, VGLL3 and TAZ S89A also both induce the myogenic regulatory factor *Myf5*. This may be important for embryonic muscle development as the somite muscle precursor cell marker Pax3 induces *Vgll3* (Lagha et al., 2010). Pax3-positive cells then become myoblasts by expressing *Myf5*. Intriguingly, a key enhancer of *Myf5* has a TEAD-bound CATTCC/GGAATG element (Ribas et al., 2011) suggesting a Pax3-Vgll3-Tead-Myf5 signalling axis that allows Pax3-positive precursors to turn into *Myf5*-expressing myoblasts in the developing embryo. Future studies should explore this idea during in vivo embryogenesis.

Other VGLL3-regulated genes in mouse include the myokine *Flst1* (Ouchi et al., 2008) and *Egfr*, a growth factor receptor associated especially with embryonal rhabdomyosarcoma (Ganti et al., 2006). Other targets are the Wnt pathway members *Wnt7b* and *Fzd4* which is relevant given that YAP and TAZ also regulate Wnt signalling genes or are regulated by Wnt members (Park et al., 2015; Sun et al., 2017). The paired-like homeodomain transcription factors *Pitx2* and *Pitx3* which are critical for foetal and regenerative myogenesis (Knopp et al., 2013; L'Honore et al., 2014) were also expressed at lower levels in myoblasts overexpressing VGLL3, as were IGF binding proteins *IGFBP2* and *4*, that fine tune IGF-1 signalling (Allard and Duan, 2018). In summary, VGLL3 acts mainly to repress gene expression, for example on the Hippo negative feedback loop, and regulates genes such as *Myf5* that control the muscle lineage.

After analysing the molecular regulation and function of Vgll3, we tested the effect of Vgll3 gain and loss-of-function on mouse and human myoblasts, as well as the skeletal muscle phenotype of *Vgll3*$^{-/-}$ mice. Here, the most striking result is that the knock-down of *VGLL3* in human myoblasts almost completely blocks proliferation. A link between VGLL3 and proliferation at least in some cell types may explain the high expression, copy number gains and function of VGLL3 in sarcomas including rhabdomyosarcomas (Cancer Genome Atlas Research Network. Electronic address and Cancer Genome Atlas Research, 2017; Helias-Rodzewicz et al., 2010). Suppression of the Hippo negative feedback loop by VGLL3 also places VGLL3 as a promoter of proliferation. Conversely, *VGLL3* has been reported to act as a tumour suppressor in epithelial ovarian cancer (Gambaro et al., 2013). This might reflect that VGLL3 can have both proliferation promoting oncogene or pro-differentiation tumour suppressor effects. Indeed, we found that overexpression of *VGLL3* at a later time point promotes the differentiation of both mouse and human myoblasts. This is reminiscent of TAZ (Mohamed et al., 2016; Sun et al., 2017), which can also switch from a pro-proliferation to a pro-differentiation regulator.

Given the molecular regulation and function of Vgll3 and its role in myoblast proliferation and differentiation, it is surprising that *Vgll3*$^{-/-}$ mice develop apparently normally without a detectable skeletal muscle phenotype. However, a sex-linked autoimmunity phenotype was reported recently for *Vgll3*$^{-/-}$ mice (Liang et al., 2017). Reasons for the lack of a major phenotype *in vivo* could be the redundancy among Tead family-targeting transcriptional co-regulators and the potent negative feedback loop which also operates in skeletal muscle cells (Judson et al., 2012). This feedback loop also probably prevents a major phenotype when the mouse *Yap1* gene is mutated in the genome so that the serine 112 phosphorylation site is mutated into an alanine (Chen et al., 2015). Similarly, we found no overt muscle phenotype in *Wwtr*$^{-/-}$ (TAZ-null) mice (Sun et al., 2017). Redundancy between Yap, Taz and Vgll1-4 may also be important and such redundancy of functionally important genes can prevent that the mutation of a single gene causes the breakdown of an organ system. Here, a good example are the myogenic regulatory factors *MyoD1* and *Myf5*

whose individual knockout has little effect on skeletal muscle development with viable mice, but whose combined knockout essentially halts functional myogenesis (Kassar-Duchossoy et al., 2004; Rudnicki et al., 1993).

Methods

Ethics statement for animal experimentation

Mice were bred in accordance with British law under the provisions of the Animals (Scientific Procedures) Act 1986, as approved by the King's College London Ethical Review Process committee. Wildtype mice were C57BL/10. Vgll3 Knockout mice (VGLL3-DEL890INS2-EM1-B6N) were provided by the MRC (The Mary Lyon Centre, MRC Harwell Institute, UK). Vgll3 knock out mice had been engineered using the CRISPR/Cas9 technology to induce a deletion of 890 nucleotides from the *Vgll3* gene (including the functionally critical exon 2) to induce a premature stop codon and a null allele (C57BL/6NtTac genetic background).

Analysis of published datasets

We downloaded several gene expression datasets from Gene Expression Omnibus (GEO) to evaluate whether challenges or disease affect *Vgll3* expression. These include dataset GDS4932 for gene expression in synergist ablation-overloaded, hypertrophying mouse plantaris muscle (Chaillou et al., 2013), dataset GDS4924 for regeneration after cardiotoxin-induced muscle injury of mouse tibialis anterior muscle (Lukjanenko et al., 2013) and dataset GDS612 from quadriceps skeletal muscle biopsies from DMD patients and unaffected control patients (Haslett et al., 2003). Moreover, we used supplementary data files from a studies comparing resting, resistance exercise or endurance exercise-trained human muscle (Vissing and Schjerling, 2014), investigating the effect of high intensity exercise on the human muscle phosphoproteome (Hoffman et al., 2015) and investigating the effect of maximal contractions on the mouse muscle phosphoproteome (Potts et al., 2017). To examine *VGLL3* expression in cancer, we analysed gene expression in 235 rhabdomyosarcoma (RMS) patients from two publicly available datasets: containing 101 samples [Innovative Therapies for Children with Cancer/ Carte d'Identite des Tumeurs (ITTC/CIT)] (Williamson et al., 2010), and 134 RMS samples [Children's Oncology Group/Intergroup Rhabdomyosarcoma Study Group (COG/IRSG)] (Davicioni et al., 2009).

Modelling Vglls binding to TEAD4 transcription factor

The structure of Vgll3 in the Vgll3-TEAD4 complex was predicted using the Phyre2 protein fold recognition server (Kelley et al., 2015). Phyre2 predicts the three-dimensional structure of the protein using its primary sequence. A model of the TONDU motif of Vgll3 was built using homology detection methods. The homologous crystal structure of the Vgll1-TEAD4 complex (PDB ID: 5Z2Q)

was used in the prediction and the confidence score of the predicted Vgll3 model is 99.8%. In the figure, the predicted Vgll3 model was overlaid on crystal structures of the Vgll1-TEAD4 complex (PDB ID: 5Z2Q) and Vgll4-TEAD complex (PDB ID: 4LN0). Only one TEAD is shown for clarity.

Competitive binding assay

HEK293 cells were grown in RPMI supplemented with 10% FBS at 37°C in 5% CO_2. HEK293 cells were transfected with HA-TEAD2, Myc-Vgll3, as indicated. The tags were introduced to the 5' end through modification of the pCI-neo vector (Promega). Constructs were transfected using lipofectamine 2000; 24h post transfection, the cells were lyzed in buffer with 20 mM Tris pH 8.0, 150mM NaCl, 0.1% Triton X-100 and protease inhibitors. HA-TEAD2 was immunoprecipitated using anti-HA beads (SIGMA) and the co-immunoprecipitated YAP was detected using anti-YAP antibody (D8H1X, Cell Signaling). HA-TEAD2 was detected using anti-HA-HRP (Sigma) and Myc-Vgll3 was detected using clone 4A6 antibody (Millipore). For antibodies, see Supplemental Table **S8**.

Labelled human YAP (61-100) and unlabelled human VGLL3 (86-112) peptides were used. Histidine-tagged human TEAD4 (217-434) was expressed in *E.coli* and purified using IMAC and gel filtration chromatography. TEAD4 was incubated with increasing concentration of VGLL3 peptide prior to the addition of labelled YAP. After 10-minute incubation at room temperature, a native gel (10%) was run at 100V to visualize free and TEAD-bound YAP.

Proteomics

The preparation of samples and analysis was performed as described previously (Sun et al., 2017). Briefly, C2C12 cells were grown in DMEM with 10% foetal bovine serum (FBS) and 4 mM glutamine. For immunoprecipitation, 80,000 C2C12 cells were seeded per 10 cm dish. The following day, the cells were transduced with control or *Vgll3*-encoding retroviral supernatant. The next day, transduction was confirmed by green fluorescent protein (GFP) from an *IRES-eGFP* in the retroviral backbone. Successful immunoprecipitation of Flag-Vgll3 was also confirmed by IP-western blotting using anti-flag antibody (Sigma F7425) (data not shown). Cells were split either in proliferation or differentiation conditions (72 h). Proliferating or differentiated cells were then washed on ice with PBS, and collected in lysis buffer (150 mM NaCl, 20 mM Tris-HCl pH 7.5, 1% Triton X100) with 1 mM sodium orthovanadate, protease inhibitor cocktail (Sigma, p8340), and Phenylmethylsulfonyl fluoride (PMSF) (Sigma-Aldrich). Lysates were incubated for 1 h on ice and centrifuged at 14,000 rpm at 4°C for 5 min and supernatant incubated at 4°C with anti-Flag M2 magnetic beads (Sigma Aldrich, M8823). Beads were washed three times with washing buffer (150 mM NaCl; 20 mM Tris-HCL pH 7.5). Sample preparation/mass spectrometry were as described (Turriziani et al., 2014). The mass spectrometry proteomics data have been deposited to the

ProteomeXchange Consortium via the PRIDE (Perez-Riverol et al., 2015; Vizcaino et al., 2016) partner repository with the dataset identifier PXD012040.

Gene expression

Myoblasts were transduced with Vgll3 encoding retrovirus for 24 h or 48 h, with empty vector retrovirus as control. RNA was isolated using TRIzol (ThermoFisher Scientific) followed by purification and DNase digestion using RNeasy minikits (Qiagen, Venlo, Netherlands). Quantification of total RNA was performed on a Nanodrop spectrophotometer (ThermoFisher Scientific) and quality tested on an Agilent Tapestation with R6K Screentapes (RIN 7.6 -9.8). Generation of sense strand cDNA from purified total RNA followed by second strand synthesis, in vitro transcription cRNA synthesis, single stranded cDNA synthesis and RNA hydrolysis, fragmentation and labelling were according to manufacturer's instructions (GeneChip WT Plus reagent kit, Affymetrix, Santa Clara, CA). Hybridisation, washing, staining and scanning of microarrays were carried out on Affymetrix Mouse Gene 2.0 ST microarrays using a GeneChip Fluidics station 450 and GCS3000 scanner (Affymetrix®, Santa Clara, CA). Performed in triplicate at Centre for Genome Enabled Biology and Medicine (University of Aberdeen).

Data pre-processing and quality control analysis was performed using Affymetrix® Genechip® Expression Console v1.2. Probe cell intensity data on the Mouse Gene 2.0 ST array (CEL files) were processed using the RMA16 algorithm (Affymetrix, Santa Clara, CA, USA), which fits a robust linear model at probe level by employing background correction, quantile normalisation of log2 transformed data and summarisation to probe level data for primary QC analysis. Performed in triplicate at Centre for Genome Enabled Biology and Medicine (University of Aberdeen). Microarray data is available via ArrayExpress accession E-MTAB-7614.

Data were analysed in Partek® Genomics Suite®, version 6.6, build 6.15.0730 Copyright ©; 2014 (Partek Inc., St Louis, MO, USA) using a Mouse gene Gene 2.0 ST annotation file from build mm10, MoGene-2.0-st-v1.na35.mm10.transcript. Affymetrix CEL files were imported to Partek® Genomics Suite®, data processed using RMA normalisation with RMA background correction and quantile normalisation of log2 transformed data and probeset summarisation by median polish. 2-way Analysis of Variance with time point (24 h, 48 h) and transcription factor (empty vector, Vgll3, YAP1 S127A, TAZ S89A) groups and time*transcription interaction was performed to evaluate significantly differentially expressed genes. YAP1 S127A and TAZ S89A (Sun et al., 2017) were included to allow comparison between Vgll3 and these Hippo pathway TEAD co-factors. Fold change in myoblasts expressing TAZ S89A, YAP S127A or Vgll3 compared to empty vector as baseline at each time point was calculated using the geometric mean of samples in each group with significance calculated by Fishers Least significant difference. Genes with fold change ≥1.3

fold and FDR of 10% in Vgll3 versus empty vector were further evaluated. The gene expression analysis was performed with the full set of samples (Empty Vector, Vgll3) and previously published YAP1S127A and TAZ S89A (Sun et al., 2017).

Myofibre isolation and culture of mouse satellite cells

Mice aged between 8–12 weeks were killed by cervical dislocation and the extensor digitorum longus (EDL) muscles were isolated and digested as previously described (Judson et al., 2012). Freshly isolated myofibres were fixed in 4% PFA for 10 min, or plated on Matrigel and the satellite cell-derived myoblasts were then expanded using DMEM-GlutaMAX (Invitrogen), with 30% FBS (Gibco), 10% horse serum (Invitrogen Life Technologies), 1% chick embryo extract (MP), 10 ng/ml bFGF (PreproTech) and 1% penicillin/streptomycin (Sigma), again as previously described (Moyle and Zammit, 2014).

In-vitro cell culture

Immortalized human myoblasts (C25Cl48) were provided by Dr. Vincent Mouly, Institute Myology, Paris (Mamchaoui et al., 2011). Proliferating human myoblasts were maintained in skeletal muscle cell growth medium (Promo-Cell, C-23160), while murine myoblasts were cultured in DMEM with 20% FBS (Gibco). Proliferation and differentiation medium were supplemented with 50 µg/ml of Gentamycin.

Mouse C2C12 myoblasts and HEK293T cells were cultured in Dulbecco's minimum essential medium (DMEM; Sigma), supplemented with 10% FBS (Hyclone). To induce differentiation, C2C12 myoblasts were cultured in growth medium until confluence, then the medium was switched to DMEM with 2% horse serum (Hyclone).

Retroviral expression vectors

The retroviral backbone *pMSCV-puro* (Clontech) was modified to replace the puromycin selection gene with an *IRES-eGFP* to create *pMSCV-IRES-eGFP*, which served as control. Mouse *Vgll3* cDNA was cloned by RT-PCR and cloned into *pMSCV-IRES-eGFP* to generate RV Vgll3. Retrovirus was then packaged in 293T cells using standard methods. Proliferating satellite cells were transduced in 6 well plates with 500 µl of retrovirus in 1.5 ml of proliferation medium with polybrene (4 µg/ml).

Mouse *Vgll3* cDNA (Transcript variant: XM_006523098.2 that encodes a protein of 276 amino acids) was amplified by RT-PCR and cloned into *pMSCV-IRES-eGFP* to generate a 3xFlag-Vgll3 retrovirus. The human cDNA of *VGLL3* (Transcript: *VGLL3-002* encodes a protein of 320 amino acids) was cloned by RT-PCR from a plasmid provided by TransOMIC technologies (MGC premier cDNA clone for *VGLL3*: BC094780) into *pMSCV-IRES-eGFP* to generate RV VGLL3. Retrovirus

(Control: empty vector encoding only for GFP and RV VGLL3) were then packaged in Phoenix cells using standard methods. Proliferating human myoblasts were transduced in 6 well plates with 200 µl of concentrated retrovirus in 1.8 ml of proliferation medium with polybrene (8 µg/ml). Cells were expanded and GFP positive cells (transduced cells) were FAC sorted, expanded *in vitro* for a few days and stably transduced cells analysed.

siRNA-mediated gene knockdown

Transfection of siRNA into primary satellite cell-derived myoblasts was performed with Silencer select Pre-designed siRNA (Invitrogen Life Technologies) using Lipofectamine RNAiMAX. The siRNAs were: Ambion, Si Vgll3 (silencer selected siRNA ID: s91841) and Silencer Select Negative Control #2 siRNA (4390847). Satellite cells were transfected with siRNA at a final concentration of 10 nM in DMEM-GlutaMAX, 30% FBS, 10% horse serum and 1% chick embryo extract for 24 h at 37°C. Transfection of siRNA into immortalized human myoblasts (C25Cl48) was performed with FlexiTube GeneSolution (4 siRNA targeting the gene of interest) (Qiagen) using Lipofectamine RNAiMAX. The siRNAs used against VGLL3 (Hs_VGLL3_1, SI03180310, Hs_VGLL3_3, SI03236233, Hs_VGLL3_4, SI04232312, Hs_VGLL3_5, SI104277819) and the All Stars Negative control siRNA. Human myoblasts were transfected with a mix of 4 siRNA targeting VGLL3 and each individual siRNA used at a final concentration of 2 nM in skeletal muscle cell growth medium (Promo-Cell) for 24 h at 37°C.

Quantitative RT-PCR

Mouse or human myoblasts were cultured in 6-well plates in proliferation medium or switched to differentiation medium for different periods of time (12, 24, 48 or 72 h). Total RNA was extracted using the RNeasy Kit (Qiagen) and cDNA prepared from 500 ng to 1 µg of RNA with the QuantiTect Reverse Transcription Kit with genomic DNA wipeout (Qiagen). qPCR was performed on a Mx3005PQPCR system (stratagene) with Brilliant II SYBR green reagents and ROX reference dye (Stratagene) using primers shown in Supplemental Table **S9**. Relative expression between proliferating and differentiated myoblasts was measured in 3 replicates and significance was tested with a two-tailed Student's t-test using Microsoft Excel.

Isolation and culture of primary human myoblasts

Primary human myoblasts were obtained from biopsies of the vastus lateralis of consenting individuals (approved by the UK National Health Service Ethics Committee (London Research Ethics Committee; reference 10/H0718/10 and in accordance with the Human Tissue Act and Declaration of Helsinki). Biopsies were digested in basal medium (PromoCell containing collagenase B and dispase II) and single cells isolated via 100 µm cell strainer as previously described (Agley et al., 2015). Adherent cells were cultured for 7 days in skeletal muscle cell

growth medium (PromoCell, Heidelberg, Germany) and the NCAM/CD56+ myogenic population collected via magnetic activated cell sorting (MACS).

Muscle cryosectioning and immunolabeling

EDL and Soleus muscles were harvested and frozen in liquid nitrogen cooled isopentane. Frozen sections (10µm) were cut on a cryostat, then dried and kept at -80°C before analysis (Ortuste Quiroga et al., 2016). Slides were allowed to warm up at room temperature, washed with PBS for 5 min and then blocked in 5% goat serum, 0.5% BSA and 0.2% triton X-100/PBS for 30 min. Primary antibodies (Supplemental Table **S8**) were prepared in blocking solution and incubated overnight at 4°C. Sections were washed in 0.05% Tween 20/PBS and secondary antibodies (Molecular Probes) (1/500) were prepared in blocking solution and applied for 1 h at room temperature. Preparations were then washed in 0.05% Tween/PBS and then incubated in DAPI (300µM) for 10 min, washed in PBS and mounted in Dako fluorescence mounting medium.

Immunolabelling of cells

EdU incorporation was performed using a Click-iT EdU Imaging Kit (Invitrogen Life Technologies) as per manufacturer's instructions. Primary murine satellite cell-derived myoblasts and C2C12 myoblasts were immunolabelled as previously described (Judson et al., 2012). Briefly, fixed myoblasts were permeabilised with 0.5% Triton X-100/PBS for 5 min at room temperature and blocked with 5% goat serum/PBS for 60 min at room temperature. Primary antibodies (e.g. anti-Flag (F1804, Sigma), anti-MyHC (MF20, DSHB) and anti-Myogenin (F5D, DSHB) are detailed in **Table S1**) were applied overnight at 4°C, washed and visualised with fluorochrome-conjugated secondary antibodies (Invitrogen) used at 1/500 for 1 h at room temperature. Preparations were then incubated in DAPI (300 µM) for 10 min and washed in PBS.

Image acquisition

Images of plated myoblasts and muscle cross sections were acquired on a Zeiss Axiovert 200 M microscope using a Zeiss AxioCam HRm and AxioVision software version 4.4 (Zeiss). Images were adjusted globally for brightness and contrast. Image of whole muscle were reconstructed from several pictures on Photoshop software (Figure 6) and analyzed (cell number counting, muscle fibre area, Ferret diameter) with ImageJ software.

Statistical testing

Cells in multiple unit areas per experimental condition well were analyzed, and all data from each of at least 3 mice or independent wells were expressed as a mean ± SEM. Significant difference (p <0.05) between control and a test sample was determined using a two-tailed t-test in Excel (Microsoft).

Acknowledgements

We are grateful to the MRC Harwell facility for generating and providing *Vgll3*$^{-/-}$ mice and Annett Riermeier for mouse phenotyping. We thank Dr. Vincent Mouly (Institute Myology, Paris, France) for human immortalised myoblasts.

Conflicts of Interest

The authors declare no potential conflicts of interest.

Funding

NF was initially funded by the European Union's Seventh Framework Programme for research, technological development and demonstration under grant agreement number 262948–2 (BIODESIGN), and then supported by the KHP R&D Challenge Fund (R151006) and the Medical Research Council (MR/P023215/1). AM was funded initially by Sarcoma UK (grant number: SUK09.2015) and then supported by funding from Postdoctoral Fellowship Program (Helmholtz Center, Munich, Germany). CS was funded by MRC grant G11001931 to HW and PSZ, and then BIODESIGN. JP is in receipt of a Wellcome Trust PhD Studentship (WT - 203949/Z/16/Z). The Zammit laboratory was additionally supported by Association Francaise contre les Myopathies (17865). This research is also supported by the Agency for Science, Technology, and Research (A*STAR), Singapore.

Data Availability

Microarray data is available via ArrayExpress accession E-MTAB-7614. The mass spectrometry proteomics data have been deposited to the ProteomeXchange Consortium via the PRIDE (Perez-Riverol et al., 2015; Vizcaino et al., 2016) partner repository with the dataset identifier PXD012040.

References

Agley, C. C., Rowlerson, A. M., Velloso, C. P., Lazarus, N. L. and Harridge, S. D. R. (2015). Isolation and quantitative immunocytochemical characterization of primary myogenic cells and fibroblasts from human skeletal muscle. *J Vis Exp*, 52049.

Akaike, K., Suehara, Y., Kohsaka, S., Hayashi, T., Tanabe, Y., Kazuno, S., Mukaihara, K., Toda-Ishii, M., Kurihara, T., Kim, Y. et al. (2018). PPP2R1A

regulated by PAX3/FOXO1 fusion contributes to the acquisition of aggressive behavior in PAX3/FOXO1-positive alveolar rhabdomyosarcoma. *Oncotarget* **9**, 25206-25215.

Allard, J. B. and Duan, C. (2018). IGF-Binding Proteins: Why Do They Exist and Why Are There So Many? *Front Endocrinol (Lausanne)* **9**, 117.

Benhaddou, A., Keime, C., Ye, T., Morlon, A., Michel, I., Jost, B., Mengus, G. and Davidson, I. (2012). Transcription factor TEAD4 regulates expression of myogenin and the unfolded protein response genes during C2C12 cell differentiation. *Cell Death Differ* **19**, 220-31.

Bernard, F., Kasherov, P., Grenetier, S., Dutriaux, A., Zider, A., Silber, J. and Lalouette, A. (2009). Integration of differentiation signals during indirect flight muscle formation by a novel enhancer of Drosophila vestigial gene. *Dev Biol* **332**, 258-72.

Bertrand, A. T., Ziaei, S., Ehret, C., Duchemin, H., Mamchaoui, K., Bigot, A., Mayer, M., Quijano-Roy, S., Desguerre, I., Laine, J. et al. (2014). Cellular microenvironments reveal defective mechanosensing responses and elevated YAP signaling in LMNA-mutated muscle precursors. *J Cell Sci* **127**, 2873-84.

Brown, S. D. and Moore, M. W. (2012). The International Mouse Phenotyping Consortium: past and future perspectives on mouse phenotyping. *Mamm Genome* **23**, 632-40.

Cancer Genome Atlas Research Network. Electronic address, e. d. s. c. and Cancer Genome Atlas Research, N. (2017). Comprehensive and Integrated Genomic Characterization of Adult Soft Tissue Sarcomas. *Cell* **171**, 950-965 e28.

Cao, L., Yu, Y., Bilke, S., Walker, R. L., Mayeenuddin, L. H., Azorsa, D. O., Yang, F., Pineda, M., Helman, L. J. and Meltzer, P. S. (2010). Genome-wide identification of PAX3-FKHR binding sites in rhabdomyosarcoma reveals candidate target genes important for development and cancer. *Cancer Res.* **70**, 6497-6508.

Chaillou, T., Lee, J. D., England, J. H., Esser, K. A. and McCarthy, J. J. (2013). Time course of gene expression during mouse skeletal muscle hypertrophy. *Journal of applied physiology (Bethesda, Md : 1985)* **115**, 1065-74.

Chen, H. H., Maeda, T., Mullett, S. J. and Stewart, A. F. (2004). Transcription cofactor Vgl-2 is required for skeletal muscle differentiation. *Genesis* **39**, 273-9.

Chen, Q., Zhang, N., Xie, R., Wang, W., Cai, J., Choi, K.-S., David, K. K., Huang, B., Yabuta, N., Nojima, H. et al. (2015). Homeostatic control of Hippo signaling activity revealed by an endogenous activating mutation in YAP. *Genes Dev* **29**, 1285-97.

Davicioni, E., Anderson, M. J., Finckenstein, F. G., Lynch, J. C., Qualman, S. J., Shimada, H., Schofield, D. E., Buckley, J. D., Meyer, W. H., Sorensen, P. H. et al. (2009). Molecular classification of rhabdomyosarcoma--genotypic and phenotypic determinants of diagnosis: a report from the Children's Oncology Group. *Am.J.Pathol.* **174**, 550-564.

G-TEx-Consortium. (2015). Human genomics. The Genotype-Tissue Expression (GTEx) pilot analysis: multitissue gene regulation in humans. *Science* **348**, 648-60.

Gabriel, B. M., Hamilton, D. L., Tremblay, A. M. and Wackerhage, H. (2016). The Hippo signal transduction network for exercise physiologists. *Journal of applied physiology (Bethesda, Md : 1985)* **120**, 1105-17.

Gambaro, K., Quinn, M. C. J., Wojnarowicz, P. M., Arcand, S. L., de Ladurantaye, M., Barres, V., Ripeau, J.-S., Killary, A. M., Davis, E. C., Lavoie, J. et al. (2013). VGLL3 expression is associated with a tumor suppressor phenotype in epithelial ovarian cancer. *Mol Oncol* **7**, 513-30.

Ganti, R., Skapek, S. X., Zhang, J., Fuller, C. E., Wu, J., Billups, C. A., Breitfeld, P. P., Dalton, J. D., Meyer, W. H. and Khoury, J. D. (2006). Expression and genomic status of EGFR and ErbB-2 in alveolar and embryonal rhabdomyosarcoma. *Mod Pathol* **19**, 1213-20.

Goodman, C. A., Dietz, J. M., Jacobs, B. L., McNally, R. M., You, J. S. and Hornberger, T. A. (2015). Yes-Associated Protein is up-regulated by mechanical overload and is sufficient to induce skeletal muscle hypertrophy. *FEBS Lett* **589**, 1491-7.

Gunther, S., Mielcarek, M., Kruger, M. and Braun, T. (2004). VITO-1 is an essential cofactor of TEF1-dependent muscle-specific gene regulation. *Nucleic Acids Res* **32**, 791-802.

Halder, G. and Carroll, S. B. (2001). Binding of the Vestigial co-factor switches the DNA-target selectivity of the Scalloped selector protein. *Development* **128**, 3295-3305.

Halder, G., Polaczyk, P., Kraus, M. E., Hudson, A., Kim, J., Laughon, A. and Carroll, S. (1998). The Vestigial and Scalloped proteins act together to directly regulate wing-specific gene expression in Drosophila. *Genes Dev.* **12**, 3900-3909.

Hansen, C. G., Moroishi, T. and Guan, K.-L. (2015). YAP and TAZ: a nexus for Hippo signaling and beyond. *Trends Cell Biol* **25**, 499-513.

Haslett, J. N., Sanoudou, D., Kho, A. T., Han, M., Bennett, R. R., Kohane, I. S., Beggs, A. H. and Kunkel, L. M. (2003). Gene expression profiling of Duchenne muscular dystrophy skeletal muscle. *Neurogenetics* **4**, 163-71.

Helias-Rodzewicz, Z., Perot, G., Chibon, F., Ferreira, C., Lagarde, P., Terrier, P., Coindre, J. M. and Aurias, A. (2010). YAP1 and VGLL3, encoding two cofactors of TEAD transcription factors, are amplified and overexpressed in a subset of soft tissue sarcomas. *Genes Chromosomes Cancer* **49**, 1161-71.

Hoffman, N. J., Parker, B. L., Chaudhuri, R., Fisher-Wellman, K. H., Kleinert, M., Humphrey, S. J., Yang, P., Holliday, M., Trefely, S., Fazakerley, D. J. et al. (2015). Global Phosphoproteomic Analysis of Human Skeletal Muscle Reveals a Network of Exercise-Regulated Kinases and AMPK Substrates. *Cell Metab* **22**, 922-35.

Honda, M., Hidaka, K., Fukada, S.-I., Sugawa, R., Shirai, M., Ikawa, M. and Morisaki, T. (2017). Vestigial-like 2 contributes to normal muscle fiber type distribution in mice. *Sci Rep* **7**, 7168.

Jiao, S., Wang, H., Shi, Z., Dong, A., Zhang, W., Song, X., He, F., Wang, Y., Zhang, Z., Wang, W. et al. (2014). A peptide mimicking VGLL4 function acts as a YAP antagonist therapy against gastric cancer. *Cancer Cell* **25**, 166-80.

Judson, R. N., Gray, S. R., Walker, C., Carroll, A. M., Itzstein, C., Lionikas, A., Zammit, P. S., De Bari, C. and Wackerhage, H. (2013). Constitutive expression of Yes-associated protein (Yap) in adult skeletal muscle fibres induces muscle atrophy and myopathy. *PLoS ONE* **8**, e59622.

Judson, R. N., Tremblay, A. M., Knopp, P., White, R. B., Urcia, R., De Bari, C., Zammit, P. S., Camargo, F. D. and Wackerhage, H. (2012). The Hippo pathway member Yap plays a key role in influencing fate decisions in muscle satellite cells. *J Cell Sci* **125**, 6009-19.

Kassar-Duchossoy, L., Gayraud-Morel, B., Gomes, D., Rocancourt, D., Buckingham, M., Shinin, V. and Tajbakhsh, S. (2004). Mrf4 determines skeletal muscle identity in Myf5:Myod double-mutant mice. *Nature* **431**, 466-71.

Kelley, L. A., Mezulis, S., Yates, C. M., Wass, M. N. and Sternberg, M. J. (2015). The Phyre2 web portal for protein modeling, prediction and analysis. *Nat Protoc* **10**, 845-58.

Knopp, P., Figeac, N., Fortier, M., Moyle, L. and Zammit, P. S. (2013). Pitx genes are redeployed in adult myogenesis where they can act to promote myogenic differentiation in muscle satellite cells. *Dev Biol* **377**, 293-304.

Koontz, L. M., Liu-Chittenden, Y., Yin, F., Zheng, Y., Yu, J., Huang, B., Chen, Q., Wu, S. and Pan, D. (2013). The Hippo effector Yorkie controls normal tissue growth by antagonizing scalloped-mediated default repression. *Dev Cell* **25**, 388-401.

L'Honore, A., Commere, P.-H., Ouimette, J.-F., Montarras, D., Drouin, J. and Buckingham, M. (2014). Redox regulation by Pitx2 and Pitx3 is critical for fetal myogenesis. *Dev Cell* **29**, 392-405.

Lagha, M., Sato, T., Regnault, B., Cumano, A., Zuniga, A., Licht, J., Relaix, F. and Buckingham, M. (2010). Transcriptome analyses based on genetic screens for Pax3 myogenic targets in the mouse embryo. *BMC.Genomics* **11**, 696.

Liang, Y., Tsoi, L. C., Xing, X., Beamer, M. A., Swindell, W. R., Sarkar, M. K., Berthier, C. C., Stuart, P. E., Harms, P. W., Nair, R. P. et al. (2017). A gene network regulated by the transcription factor VGLL3 as a promoter of sex-biased autoimmune diseases. *Nat Immunol* **18**, 152-160.

Lukjanenko, L., Brachat, S., Pierrel, E., Lach-Trifilieff, E. and Feige, J. N. (2013). Genomic profiling reveals that transient adipogenic activation is a hallmark of mouse models of skeletal muscle regeneration. *PLoS One* **8**, e71084.

Maeda, T., Chapman, D. L. and Stewart, A. F. (2002). Mammalian vestigial-like 2, a cofactor of TEF-1 and MEF2 transcription factors that promotes skeletal muscle differentiation. *J Biol Chem* **277**, 48889-98.

Mamchaoui, K., Trollet, C., Bigot, A., Negroni, E., Chaouch, S., Wolff, A., Kandalla, P. K., Marie, S., Di Santo, J., St Guily, J. L. et al. (2011). Immortalized pathological human myoblasts: towards a universal tool for the study of neuromuscular disorders. *Skelet Muscle* **1**, 34.

Mielcarek, M., Gunther, S., Kruger, M. and Braun, T. (2002). VITO-1, a novel vestigial related protein is predominantly expressed in the skeletal muscle lineage. *Mech Dev* **119 Suppl 1**, S269-74.

Mielcarek, M., Piotrowska, I., Schneider, A., Gunther, S. and Braun, T. (2009). VITO-2, a new SID domain protein, is expressed in the myogenic lineage during early mouse embryonic development. *Gene Expr Patterns* **9**, 129-37.

Missiaglia, E., Williamson, D., Chisholm, J., Wirapati, P., Pierron, G., Petel, F., Concordet, J. P., Thway, K., Oberlin, O., Pritchard-Jones, K. et al. (2012). PAX3/FOXO1 fusion gene status is the key prognostic molecular marker in rhabdomyosarcoma and significantly improves current risk stratification. *J.Clin.Oncol.* **30**, 1670-1677.

Mohamed, A., Sun, C., De Mello, V., Selfe, J., Missiaglia, E., Shipley, J., Murray, G. I., Zammit, P. S. and Wackerhage, H. (2016). The Hippo effector TAZ (WWTR1) transforms myoblasts and TAZ abundance is associated with reduced survival in embryonal rhabdomyosarcoma. *J Pathol* **240**, 3-14.

Moyle, L. A. and Zammit, P. S. (2014). Isolation, culture and immunostaining of skeletal muscle fibres to study myogenic progression in satellite cells. *Methods Mol Biol* **1210**, 63-78.

Ortuste Quiroga, H. P., Goto, K. and Zammit, P. S. (2016). Isolation, Cryosection and Immunostaining of Skeletal Muscle. *Methods Mol Biol* **1460**, 85-100.

Ouchi, N., Oshima, Y., Ohashi, K., Higuchi, A., Ikegami, C., Izumiya, Y. and Walsh, K. (2008). Follistatin-like 1, a secreted muscle protein, promotes endothelial cell function and revascularization in ischemic tissue through a nitric-oxide synthase-dependent mechanism. *J Biol Chem* **283**, 32802-11.

Park, H. W., Kim, Y. C., Yu, B., Moroishi, T., Mo, J. S., Plouffe, S. W., Meng, Z., Lin, K. C., Yu, F. X., Alexander, C. M. et al. (2015). Alternative Wnt Signaling Activates YAP/TAZ. *Cell* **162**, 780-94.

Perez-Riverol, Y., Alpi, E., Wang, R., Hermjakob, H. and Vizcaino, J. A. (2015). Making proteomics data accessible and reusable: current state of proteomics databases and repositories. *Proteomics* **15**, 930-49.

Piccolo, S., Dupont, S. and Cordenonsi, M. (2014). The biology of YAP/TAZ: hippo signaling and beyond. *Physiol Rev* **94**, 1287-312.

Pimmett, V. L., Deng, H., Haskins, J. A., Mercier, R. J., LaPointe, P. and Simmonds, A. J. (2017). The activity of the Drosophila Vestigial protein is modified by Scalloped-dependent phosphorylation. *Dev Biol* **425**, 58-69.

Pobbati, A. V., Chan, S. W., Lee, I., Song, H. and Hong, W. (2012). Structural and functional similarity between the Vgll1-TEAD and the YAP-TEAD complexes. *Structure* **20**, 1135-40.

Potts, G. K., McNally, R. M., Blanco, R., You, J.-S., Hebert, A. S., Westphall, M. S., Coon, J. J. and Hornberger, T. A. (2017). A map of the phosphoproteomic alterations that occur after a bout of maximal-intensity contractions. *J Physiol* **595**, 5209-5226.

Ribas, R., Moncaut, N., Siligan, C., Taylor, K., Cross, J. W., Rigby, P. W. and Carvajal, J. J. (2011). Members of the TEAD family of transcription factors regulate the expression of Myf5 in ventral somitic compartments. *Dev.Biol.* **355**, 372-380.

Rudnicki, M. A., Schnegelsberg, P. N., Stead, R. H., Braun, T., Arnold, H. H. and Jaenisch, R. (1993). MyoD or Myf-5 is required for the formation of skeletal muscle. *Cell* **75**, 1351-1359.

Shern, J. F., Chen, L., Chmielecki, J., Wei, J. S., Patidar, R., Rosenberg, M., Ambrogio, L., Auclair, D., Wang, J., Song, Y. K. et al. (2014). Comprehensive genomic analysis of rhabdomyosarcoma reveals a landscape of alterations affecting a common genetic axis in fusion-positive and fusion-negative tumors. *Cancer Discov* **4**, 216-31.

Simon, E., Faucheux, C., Zider, A., Theze, N. and Thiebaud, P. (2016). From vestigial to vestigial-like: the Drosophila gene that has taken wing. *Development genes and evolution* **226**, 297-315.

Simon, E., Theze, N., Fedou, S., Thiebaud, P. and Faucheux, C. (2017). Vestigial-like 3 is a novel Ets1 interacting partner and regulates trigeminal nerve formation and cranial neural crest migration. *Biol Open* **6**, 1528-1540.

Slemmons, K. K., Crose, L. E. S., Rudzinski, E., Bentley, R. C. and Linardic, C. M. (2015). Role of the YAP Oncoprotein in Priming Ras-Driven Rhabdomyosarcoma. *PLoS One* **10**, e0140781.

Sun, C., De Mello, V., Mohamed, A., Ortuste Quiroga, H. P., Garcia-Munoz, A., Al Bloshi, A., Tremblay, A. M., von Kriegsheim, A., Collie-Duguid, E., Vargesson, N. et al. (2017). Common and Distinctive Functions of the Hippo Effectors Taz and Yap in Skeletal Muscle Stem Cell Function. *Stem Cells* **35**, 1958-1972.

Tremblay, A. M. and Camargo, F. D. (2012). Hippo signaling in mammalian stem cells. *Semin.Cell Dev.Biol.* **23**, 818-826.

Tremblay, A. M., Missiaglia, E., Galli, G. G., Hettmer, S., Urcia, R., Carrara, M., Judson, R. N., Thway, K., Nadal, G., Selfe, J. L. et al. (2014). The Hippo transducer YAP1 transforms activated satellite cells and is a potent effector of embryonal rhabdomyosarcoma formation. *Cancer Cell* **26**, 273-87.

Tsika, R. W., Schramm, C., Simmer, G., Fitzsimons, D. P., Moss, R. L. and Ji, J. (2008). Overexpression of TEAD-1 in Transgenic Mouse Striated Muscles Produces a Slower Skeletal Muscle Contractile Phenotype. *J.Biol.Chem.* **283**, 36154-36167.

Turriziani, B., Garcia-Munoz, A., Pilkington, R., Raso, C., Kolch, W. and von Kriegsheim, A. (2014). On-beads digestion in conjunction with data-dependent mass spectrometry: a shortcut to quantitative and dynamic interaction proteomics. *Biology (Basel)* **3**, 320-32.

Vaudin, P., Delanoue, R., Davidson, I., Silber, J. and Zider, A. (1999). TONDU (TDU), a novel human protein related to the product of vestigial (vg) gene of Drosophila melanogaster interacts with vertebrate TEF factors and substitutes for Vg function in wing formation. *Development* **126**, 4807-4816.

Vissing, K. and Schjerling, P. (2014). Simplified data access on human skeletal muscle transcriptome responses to differentiated exercise. *Scientific data* **1**, 140041.

Vizcaino, J. A., Csordas, A., Del-Toro, N., Dianes, J. A., Griss, J., Lavidas, I., Mayer, G., Perez-Riverol, Y., Reisinger, F., Ternent, T. et al. (2016). 2016 update of the PRIDE database and its related tools. *Nucleic Acids Res* **44**, 11033.

Wackerhage, H., Del Re, D. P., Judson, R. N., Sudol, M. and Sadoshima, J. (2014). The Hippo signal transduction network in skeletal and cardiac muscle. *Sci Signal* **7**, re4.

Wang, P., Bouwman, F. G. and Mariman, E. C. M. (2009). Generally detected proteins in comparative proteomics--a matter of cellular stress response? *Proteomics* **9**, 2955-66.

Watt, K. I., Judson, R., Medlow, P., Reid, K., Kurth, T. B., Burniston, J. G., Ratkevicius, A., De Bari, C. and Wackerhage, H. (2010). Yap is a novel regulator of C2C12 myogenesis. *Biochem Biophys Res Commun* **393**, 619-24.

Watt, K. I., Turner, B. J., Hagg, A., Zhang, X., Davey, J. R., Qian, H., Beyer, C., Winbanks, C. E., Harvey, K. F. and Gregorevic, P. (2015). The Hippo pathway effector YAP is a critical regulator of skeletal muscle fibre size. *Nat Commun* **6**, 6048.

Williamson, D., Missiaglia, E., de, R. A., Pierron, G., Thuille, B., Palenzuela, G., Thway, K., Orbach, D., Lae, M., Freneaux, P. et al. (2010). Fusion gene-negative alveolar rhabdomyosarcoma is clinically and molecularly indistinguishable from embryonal rhabdomyosarcoma. *J.Clin.Oncol.* **28**, 2151-2158.

Figures

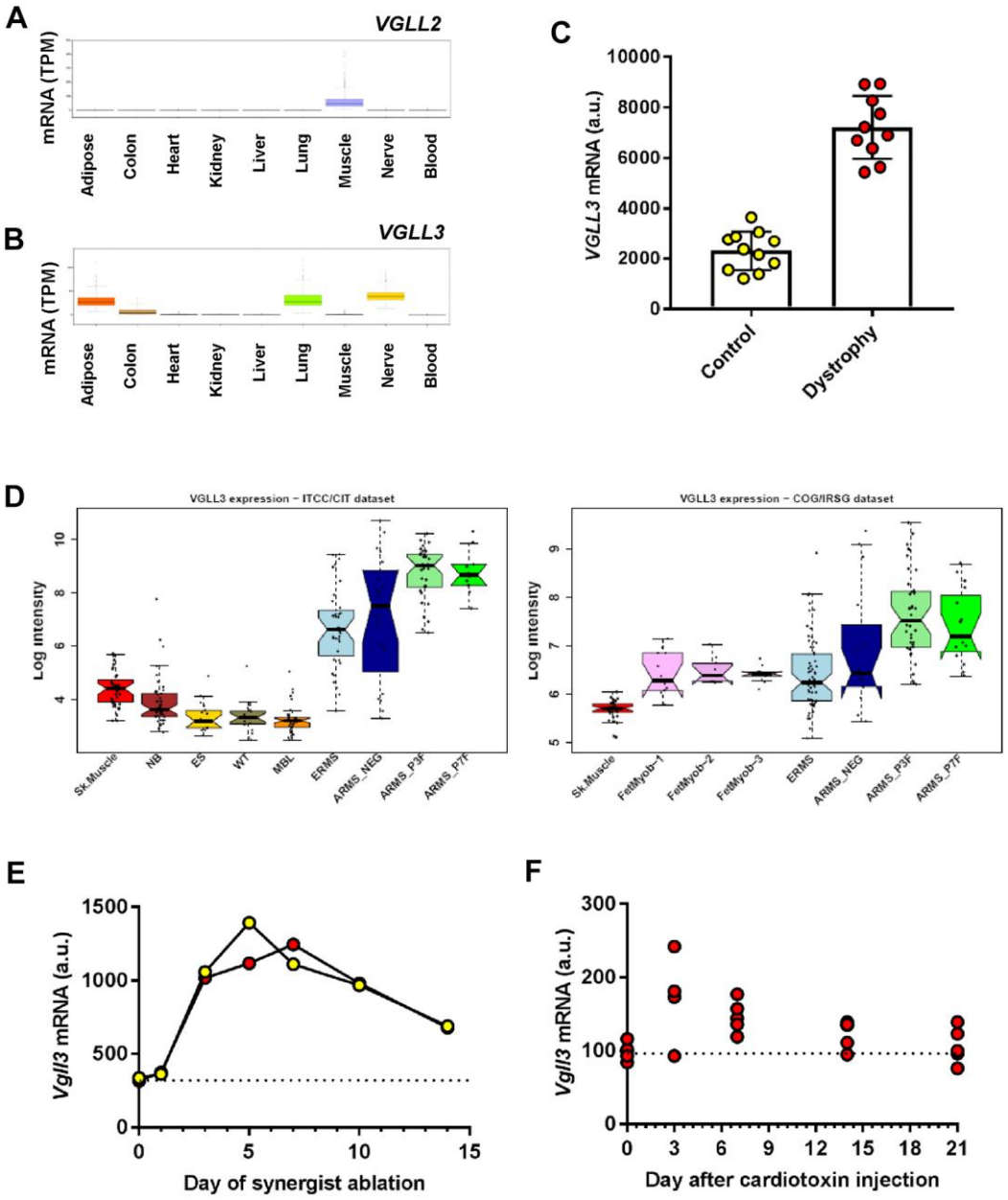

Figure 1: Vgll2 and Vgll3 expression in skeletal muscle and cancer.

(a) *VGLL2* and (**b)** *VGLL3* expression in different human tissues (G-TEx-Consortium, 2015). (**c)** *VGLL3* expression in healthy and Duchenne muscular dystrophy vastus lateralis muscle biopsy samples (Haslett et al., 2003). (**d)** VGLL3 expression in human skeletal muscle (Sk. Muscle), neuroblastoma (NB), Ewing Sarcoma (ES), embryonal rhabdomyosarcoma (ERMS), fusion gene-negative alveolar rhabdomyosarcoma (AMRS_NEG), ARMS expressing PAX3-FOXO1 (ARMS_P3F) or PAX7-FOXO1 (ARMS_P7F) fusion genes (Davicioni et al., 2009; Williamson et al., 2010). In addition VGLL3 expression in foetal myoblasts (FetMyob) at different days is shown. (**e)**

Expression of *Vgll3* mRNA after mouse synergist ablation (Chaillou et al., 2013) or (**f)** regenerating mouse tibialis anterior muscle following cardiotoxin injection (Lukjanenko et al., 2013).

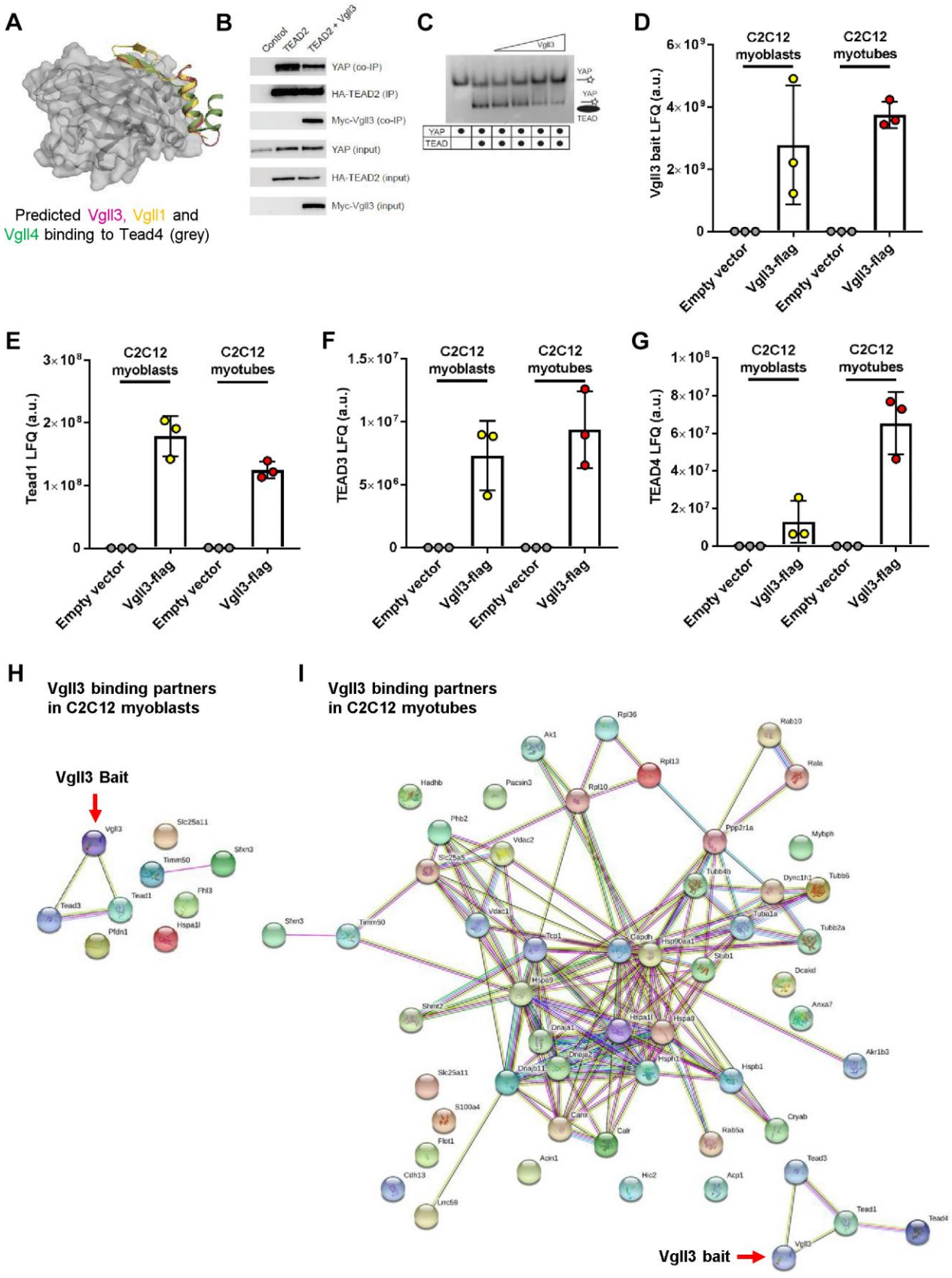

Figure 2: VGLL3 binding protein partners in murine myoblasts and myotubes

(a) Superposition of VGLL1-TEAD4 (PDB ID: 5Z2Q) and VGLL4-TEAD4 (PDB ID: 4LN0) crystal structures with the modelled VGLL3-TEAD4 structure. A surface-ribbon representation of TEAD4 is

shown in grey. (**b)** Expression of VGLL3 in HEK293 cells in an *in vitro* competition assay reduces the binding of YAP to TEAD2 suggesting competition between VGLL3 and YAP for binding to TEAD2. (**c**) Native gel showing the migration of free and TEAD4-bound labelled YAP. Only the labelled YAP is seen. Upon addition of VGLL3 peptide, the amount of TEAD4-bound YAP is reduced, with a concomitant increase in the amount of free YAP, again indicating competition between VGLL3 and YAP for binging to TEAD4. (**d)** VGLL3-flag IP proteomics shows that the Vgll3 bait is detected and (**e-g)** that VGLL3-flag binds TEAD1, TEAD3 and TEAD4 in murine C2C12 myoblasts and/or myotubes. (**h**) String analysis of VGLL3-flag binding partners identified in C2C12 myoblasts and **(i)** in C2C12 myotubes.

A

Gene	Full name	Vgll3		YAP1 S127A		TAZ S89A	
		Fold-change	*p* value	Fold-change	*p* value	Fold-change	*p* value
Vgll2	Vestigial like 2 homolog	-2.05	0.00	1.06	0.49	2.45	0.00
Wwtr1	WW domain containing transcription regulator 1	-1.35	0.00	-1.24	0.00	-1.14	0.02
Ajuba	Ajuba LIM protein	-1.76	0.00	1.54	0.00	1.62	0.00
Amotl2	Angiomotin-like 2	-1.76	0.00	1.59	0.00	1.84	0.00
Frmd6	FERM domain containing 6 , Willin	-1.54	0.00	1.49	0.00	1.21	0.00
Myf5	Myogenic factor 5	1.32	0.00	-1.05	0.37	1.45	0.00
Fstl1	Follistatin-like 1	-1.48	0.00	1.42	0.00	1.16	0.04
Egfr	Epidermal growth factor receptor	1.57	0.00	-1.06	0.50	1.16	0.09
Wnt7b	Wingless-type, member 7B	1.51	0.00	1.08	0.30	1.16	0.07
Fzd4	Frizzled homolog 4	-1.81	0.00	-1.31	0.02	-1.15	0.20
Pitx2	Paired-like homeodomain transcription factor 2	-1.57	0.00	-1.36	0.00	-1.26	0.01
Pitx3	Paired-like homeodomain transcription factor 2	-1.31	0.00	-1.07	0.15	-1.53	0.00
Igfbp2	Insulin-like growth factor binding protein 2	-2.28	0.00	-1.25	0.07	1.16	0.22
Igfbp3	Insulin-like growth factor binding protein 3	1.56	0.00	-1.23	0.06	-1.08	0.43
Igfbp4	Insulin-like growth factor binding protein 4	-1.38	0.00	-1.37	0.00	-1.48	0.00

Red >1.3 fold change; blue <-1.3 fold change

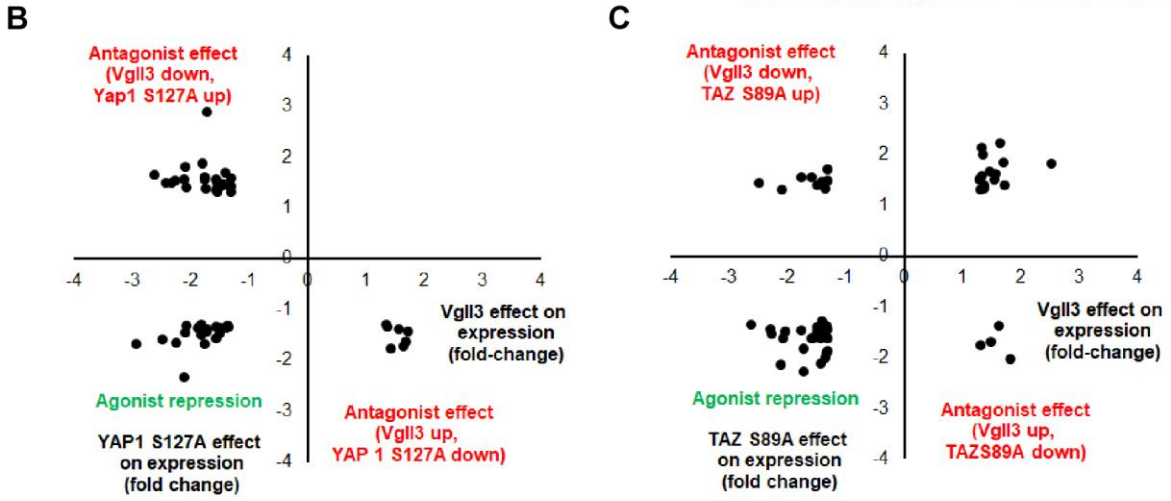

Figure 3: Transcriptomic analysis of VGLL3 target gene expression

(a) Examples of regulation of Hippo-related genes and of genes controlling muscle functions by VGLL3 versus YAP1 S127A or TAZ S89A in primary murine satellite cell-derived myoblasts at 48 h (FDR <10%). **(b and c)** In satellite cell-derived myoblasts, VGLL3 drives expression of genes that are both regulated and unregulated by YAP (**b**) or TAZ (**c**), having both agonist and antagonist effects.

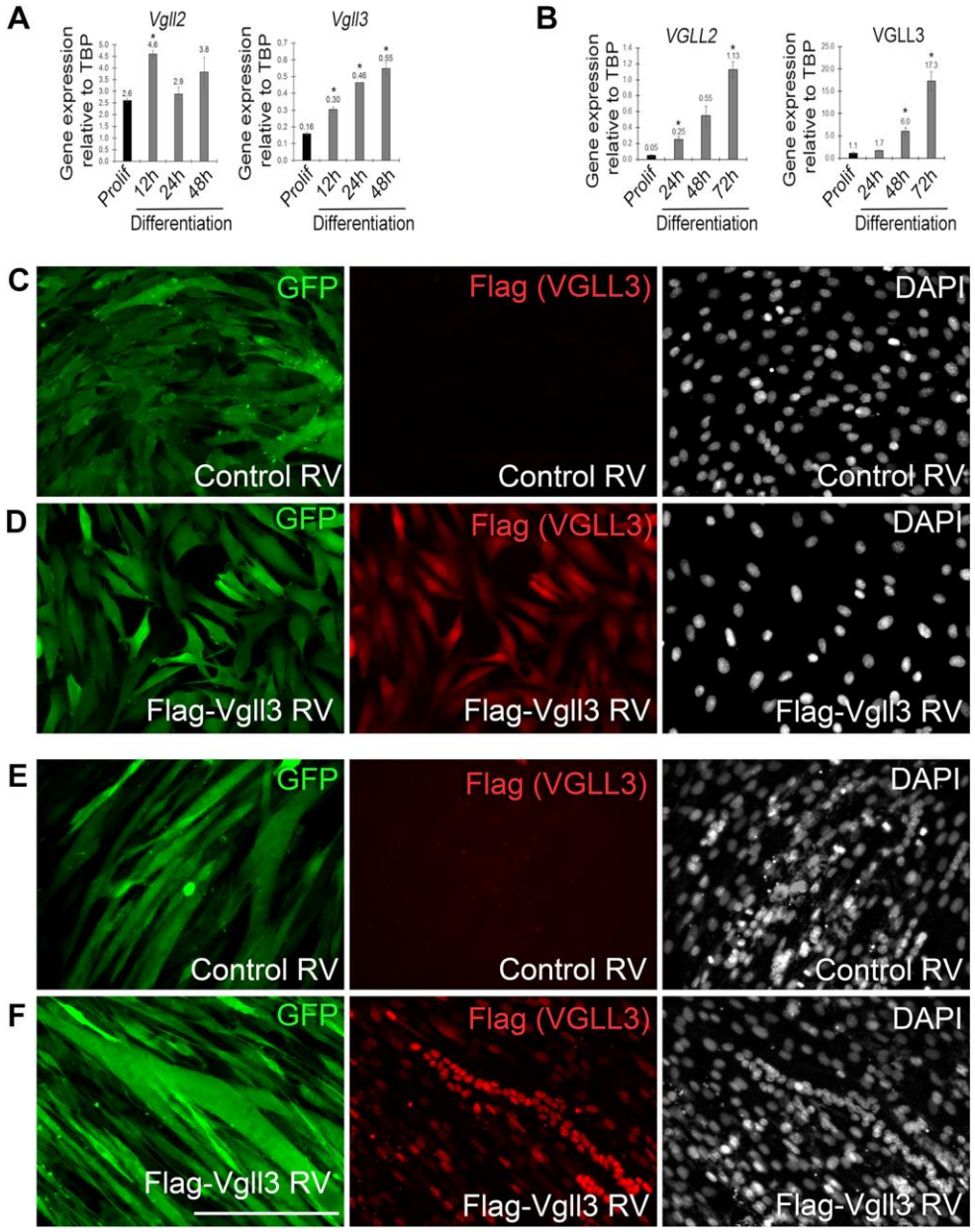

Figure 4: Vgll3 expression dynamics and localisation during myogenesis

(a) Expression of *Vgll2* and *Vgll3* analyzed by RT-qPCR in proliferating and differentiating primary mouse satellite cell-derived myoblasts or **(b)** primary human myoblasts ex vivo. **(c)** Proliferating murine C2C12 myoblasts transduced with control or (**d**) Flag-Vgll3 encoding retrovirus and immunolabelled for eGFP to identify transduced cells (from the *IRES-eGFP* in the retroviral backbone) and Flag to detect VGLL3. **(e)** Differentiated C2C12 myocytes and multinucleated myotubes transduced with control or (**f**) Flag-Vgll3 encoding retrovirus and immunolabelled for eGFP and Flag to detect VGLL3, showing clear nuclear localisation of VGLL3. Data are presented as mean ± SEM, where an asterisk indicates a significant difference (p<0.05) between proliferation and differentiation samples using a paired two-tailed t-test, where n=3 mice or independent experiments. Scale bar represents 100 µm.

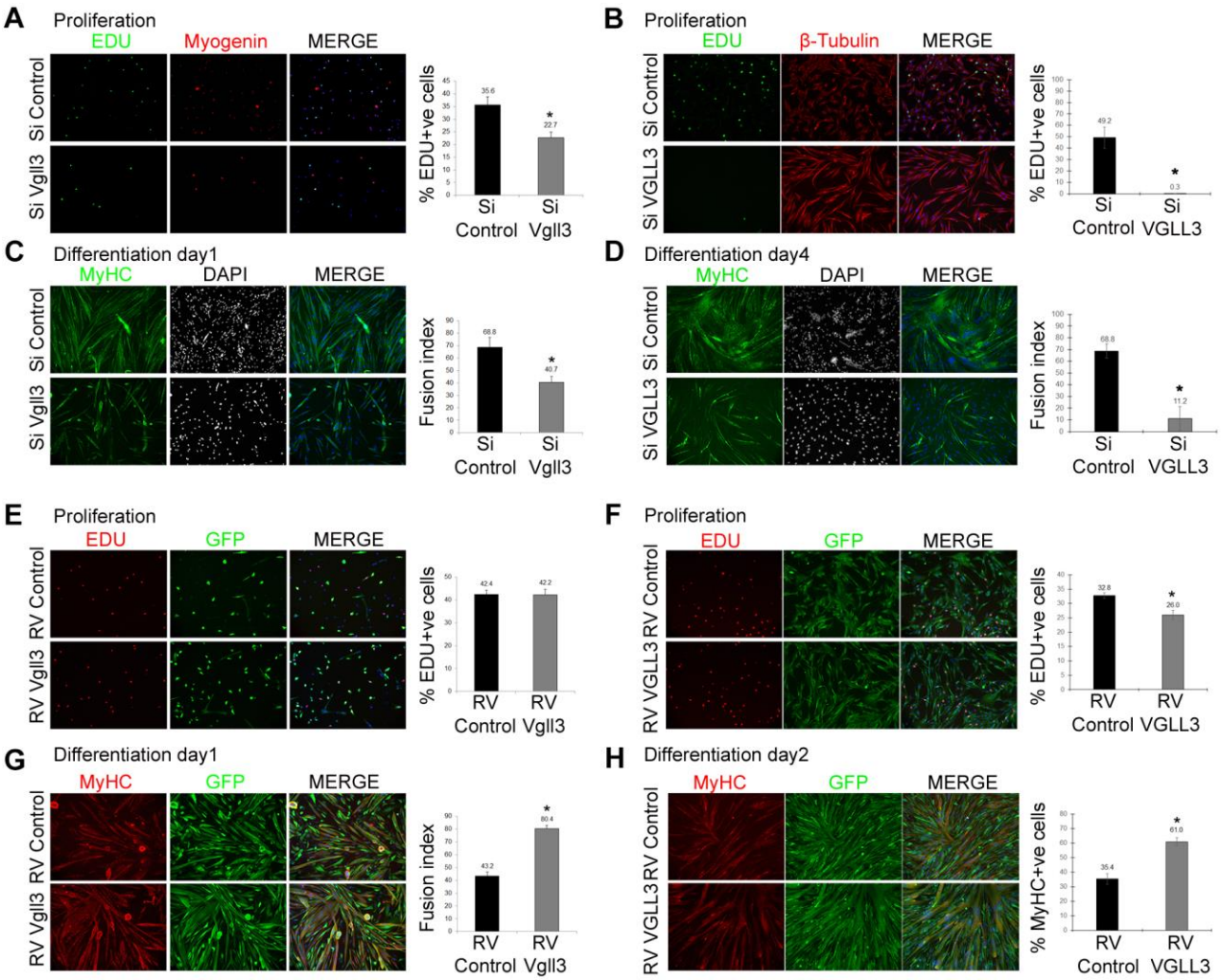

Figure 5: *Vgll3* supports proliferation and differentiation in mouse and human myoblasts.

(**a-d**) Effects of siRNA-mediated *Vgll3* knock-down on cell proliferation (**a**, **b**) and myotube formation (**c, d**) in primary murine satellite cell-derived myoblasts (**a, c**) or immortalised human C25Cl48 myoblasts (**b, d**). Proliferating mouse or human myoblasts were immunolabelled for (**a**) Myogenin or (**b**) β-tubulin and EdU incorporation measured. (**c and d)** Myotubes were visualized by MyHC immunolabeling. (**e-h**) Effects of retroviral-mediated Vgll3 overexpression on myoblast proliferation (**e, f**) and myotube formation (**g, h**) in both transiently transduced primary murine satellite cell-derived myoblasts (**e, g**) or stable *VGLL3*-expressing immortalised human C25Cl48 myoblasts (**f, h**). (**e, f**) Proliferating myoblasts were immunolabelled for GFP (to detect transduced cells from the *IRES-eGFP* in the retroviral backbone) and EdU incorporation measured, while (**g, h**) myotubes were immunolabelled for GFP and MyHC. Reduction of Vgll3 generally inhibits proliferation, while constitutive Vgll3 expression enhances myogenic differentiation. Data are presented as mean ± SEM, where an asterisk indicates a significant difference ($p < 0.05$) between test sample and control using a paired two-tailed t-test, where n=3 mice or independent experiments. Scale bar represents 100 µm

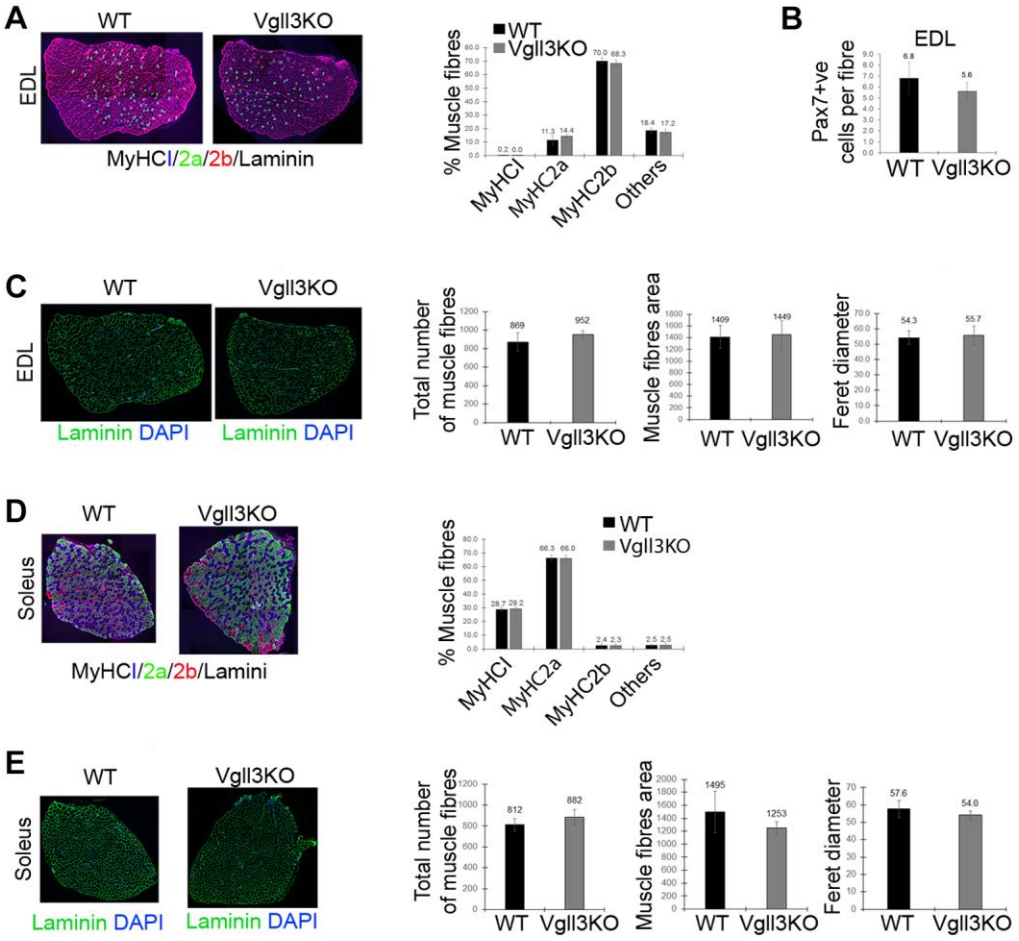

Figure 6: *Vgll3*-null mice have normal muscle structure and fibre type content

(**a**) Extensor digitorum longus (EDL) and (**d**) Soleus muscle transverse sections co-immunolabelled for MyHC I, MyHC 2a or MyHC 2b, together with laminin, from wild type or *Vgll3*$^{-/-}$ (Vgll3KO) mice. Quantification from such images reveals no changes in the proportions of each muscle fibre type. (**b)** Quantification of the number of Pax7-expressing satellite cells per isolated EDL myofibre in wild type and Vgll3KO mice. (**c**) EDL and (**e**) Soleus muscle transverse sections immunolabelled for laminin and counterstained with DAPI from wild type or *Vgll3*KO mice and corresponding quantification of the total number of myofibres per muscle, together with area and Feret diameter of muscle fibres. Data are presented as mean ± SEM, where an asterisk would indicate a significant difference (p<0.05) between a test sample and control using a unpaired two-tailed t-test with n=3 mice. Scale bar represents 50 µm.

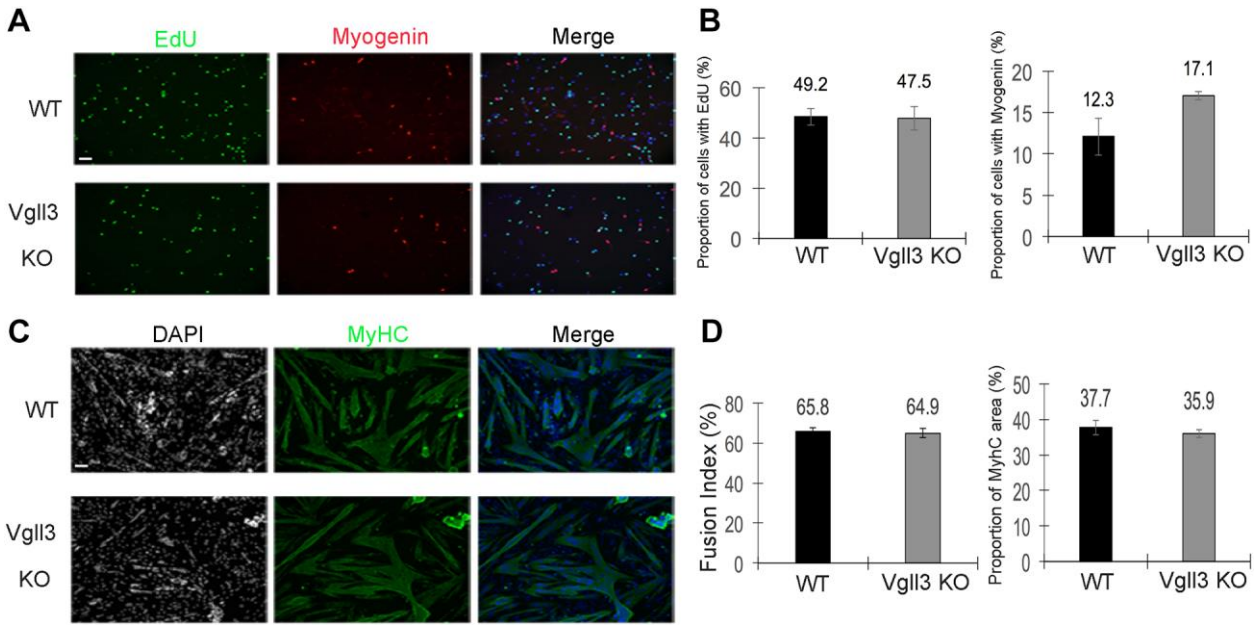

Figure 7: Loss of Vgll3 does not affect proliferation or differentiation of satellite cell-derived myoblasts

(**a**) Primary satellite cells were isolated from the EDL muscle of WT or *Vgll3*$^{-/-}$ (Vgll3 KO) mice. Myoblasts were expanded in vitro (on matrigel) in proliferation medium and pulsed with EDU for 2 h. EDU incorporation was visualised and immunolabelling for Myogenin performed. (**b**) Proliferation of *Vgll3* KO satellite cells was similar to that of wildtype controls, with 47-48% of myoblasts incorporating EDU. There was a non-significant trend for more myogenin-positive cells in the *Vgll3* KO satellite cells compared to control. (**c)** EDL Primary satellite cells of WT or *Vgll3*$^{-/-}$ (Vgll3 KO) mice were expanded *in vitro* (on matrigel) in proliferation medium and then switched to differentiation medium for one day. Cells were immunolabelled for MyHC, then fusion index and MyHC-positive area determined. (**d**) Myotube formation in Vgll3 KO satellite cells was not significantly different to wildtype control satellite cells, with a fusion index of 64.9% compared to 65.8% in controls. Data are presented as mean ± SEM, where an asterisk would indicate a significant difference (p<0.05) between a test sample and control using a unpaired two-tailed t-test with n=3 mice. Scale bar represents 50 µm.

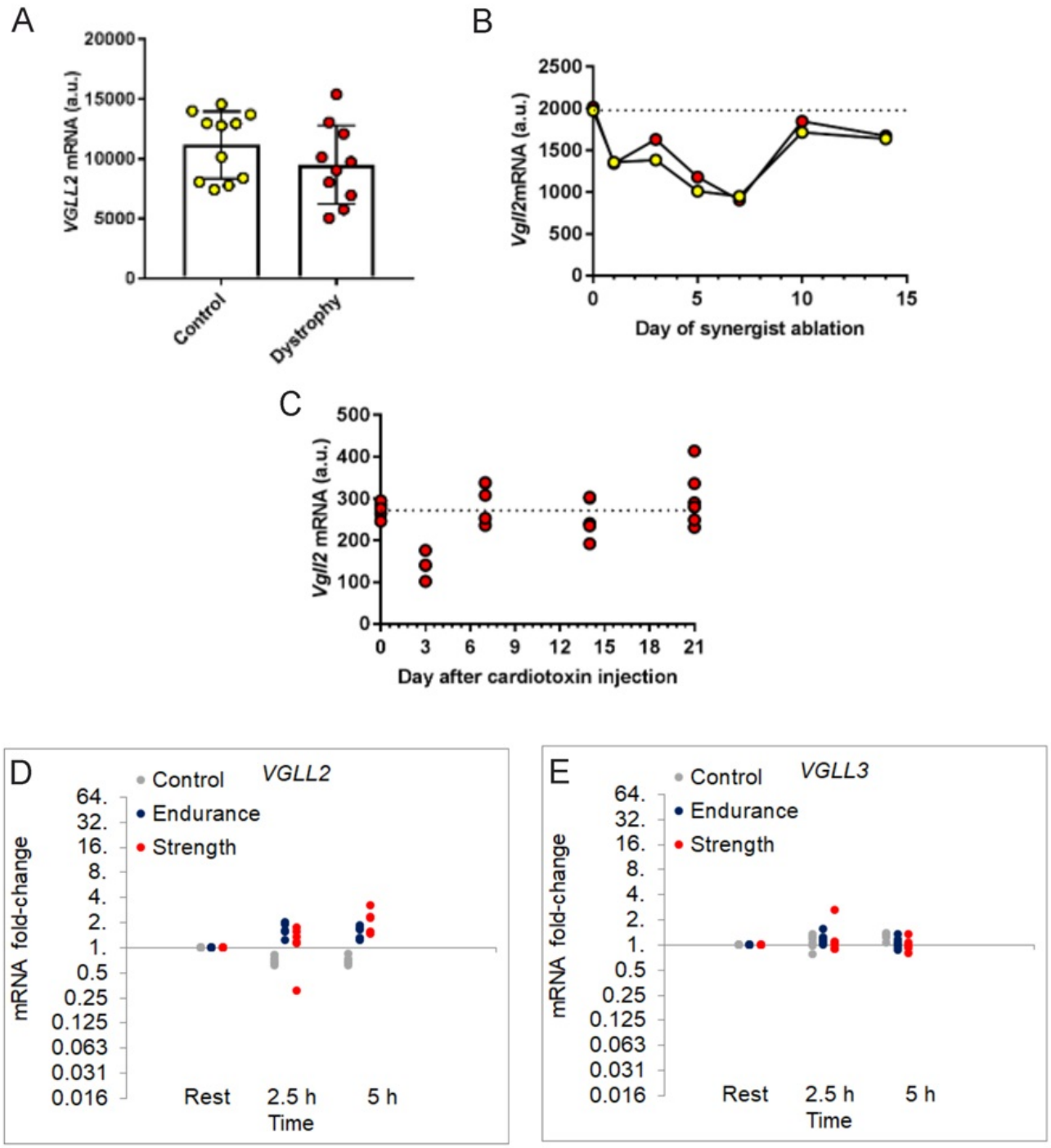

Figure S1: Expression of *Vgll2* and *Vgll3* in muscle

(A) VGLL2 expression in the quadriceps muscle of boys with Duchenne muscular dystrophy versus healthy controls (Retrieval of gene expression data from: **Haslett, J. N., Sanoudou, D., Kho, A. T., Han, M., Bennett, R. R., Kohane, I. S., Beggs, A. H. and Kunkel, L. M.** (2003). Gene expression profiling of Duchenne muscular dystrophy skeletal muscle. *Neurogenetics* **4**, 163-71).
(B) Vgll2 expression in mouse plantaris muscle overloaded through synergist ablation starting at day 0 (Retrieval of gene expression data from: **Chaillou, T., Lee, J. D., England, J. H., Esser, K. A. and McCarthy, J. J.** (2013). Time course of gene expression during mouse skeletal muscle hypertrophy. *J Appl Physiol (1985)* **115**, 1065-74).
(C) Vgll2 expression in mouse tibialis anterior muscle injured with cardiotoxin injection at day 0 (Retrieval of gene expression data from: **Lukjanenko, L., Brachat, S., Pierrel, E., Lach-Trifilieff, E. and Feige, J. N.** (2013). Genomic profiling reveals that transient adipogenic activation is a hallmark of mouse models of skeletal muscle regeneration. *PLoS ONE* **8**, e71084).
(D) *VGLL2* and **(E)** *VGLL3* expression in the vastus lateralis muscle before, 2.5 and 5 h after endurance or resistance exercise (Retrieval of gene expression data from: **Vissing, K. and Schjerling, P.** (2014). Simplified data access on human skeletal muscle transcriptome responses to differentiated exercise. *Sci Data* **1**, 140041).

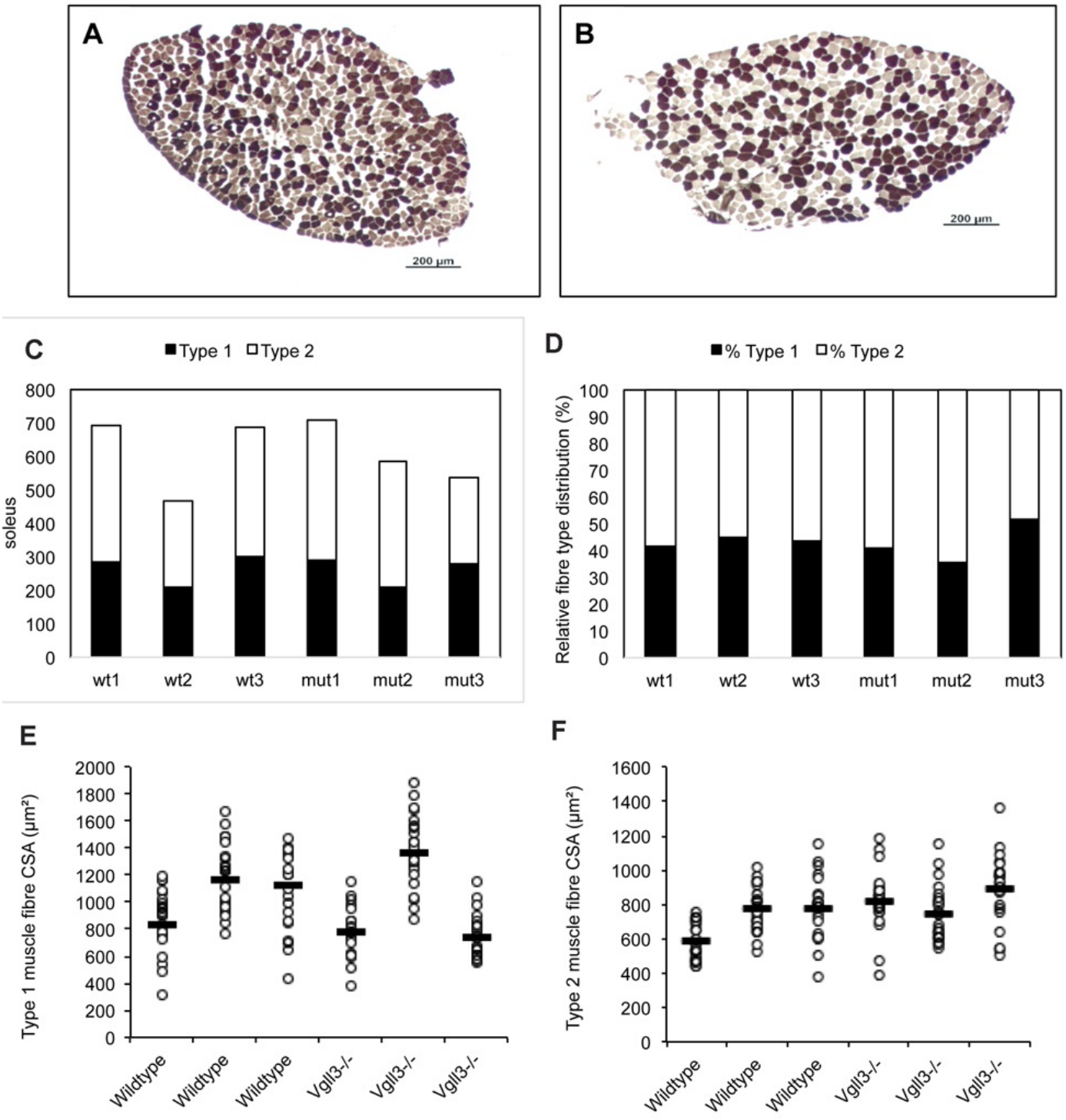

Figure S2: Vgll3 knockout does not affect muscle fibre type distribution or myofibre cross-sectional area in hind limb muscles

(**A-B**) ATPase-stained section of a wildtype soleus (**A**) or the soleus from a *Vgll3* knock out mouse (**B**).
(**C**) Absolute and (**D**) relative type 1 and type 2 (2a) fibre numbers in the soleus of wildtype (wt) and *Vgll3*$^{-/-}$(mut) mice.
(**E-F**) Type 1 and type 2 (2a) muscle fibre cross sectional area (CSA) of the gastrocnemius of wildtype and *Vgll3*$^{-/-}$ mice.

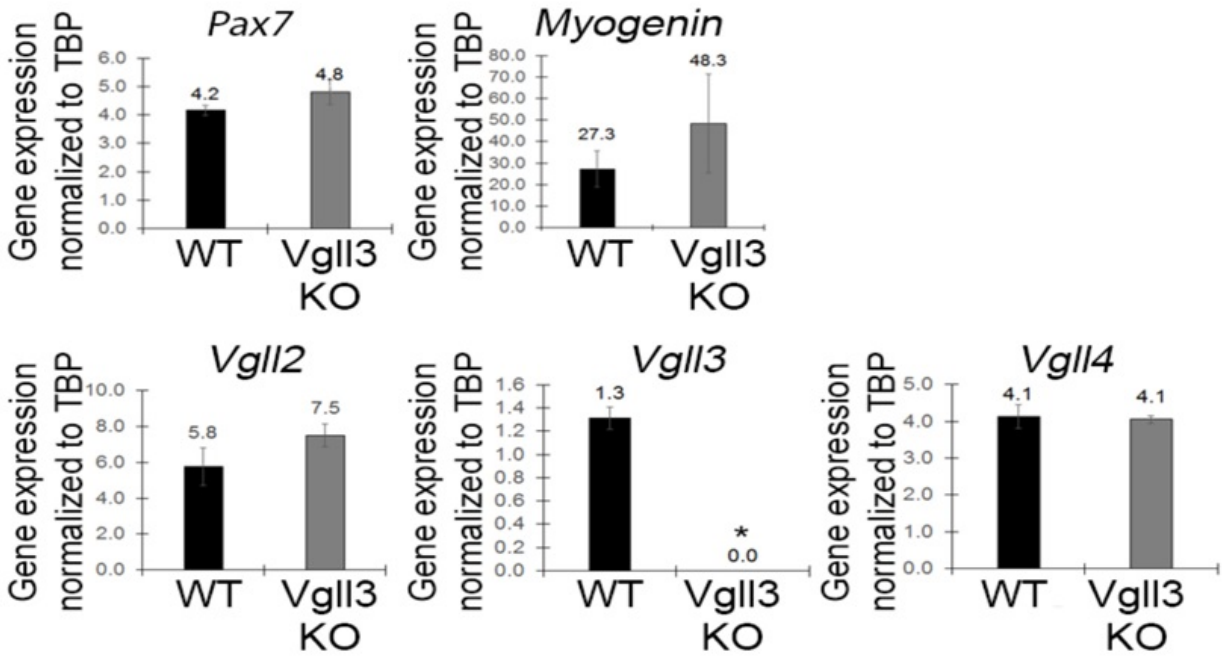

Figure S3: Vgll3 KO-derived satellite cells have unchanged gene expression
Expression of *Pax7*, *Myogenin*, *Vgll2*, *Vgll3* and *Vgll4* were analysed by RT-qPCR in proliferating satellite cells isolated from WT and *Vgll3*$^{-/-}$ (KO) mice and found not to be significantly different. Data are presented as mean ± SEM, where an asterisk would indicate a significant difference (p<0.05) between a test sample and control using a unpaired two-tailed t-test with n=3 mice.

Table S1: Proteins that bind VGLL3 in the skeletal muscle lineage
Downstream, VGLL3 binds TEAD1, TEAD3 and TEAD4 in C2C12 cells. Upstream, the key protein groups are Heat shock and related proteins, tubulins, metabolic genes and mitochondrial channels. VGLL3 targets TEAD1,3,4 transcription factors and no other transcription factors in the muscle lineage under standard cell culture conditions. The function of the upstream binding proteins is unknown.

Click here to Download Table S1

Table S2: Proteins that bind VGLL3, YAP and TAZ in C2C12 myoblasts and myotubes
(**A**) Comparison of VGLL3 with YAP and TAZ binding partners as we described in Sun, C., De Mello, V., Mohamed, A., Ortuste Quiroga, H. P., Garcia-Munoz, A., Al Bloshi, A., Tremblay, A. M., von Kriegsheim, A., Collie-Duguid, E., Vargesson, N. et al. (2017). Common and Distinctive Functions of the Hippo Effectors Taz and Yap in Skeletal Muscle Stem Cell Function. Stem Cells 35, 1958-1972. VGLL3-flag, YAP-flag and TAZ-flag all bind Tead1,3,4 in C2C12 cells.
(**B**) Whilst there is an 18.6% overlap between YAP-flag and TAZ-flag binding partners, the overlap with VGLL3-flag binding partners is only ~1%. Only 4 proteins (1.3%) bind both VGLL3-flag and YAP-flag and 3 proteins (1%) bind both VGLL3-flag and YAP-flag. Collectively this suggest that VGLL3, YAP and TAZ all target TEAD family transcription factors in C2C12 myoblasts and myotubes. However, non-transcription factor-binding partners are largely different.

Click here to Download Table S2

Table S3: Analysis of the human VGLL3 FASTA sequence led to the prediction of a MQDSLEVTL nuclear export signal which was fully conserved between man, chimpanzee, cat and mouse
(**A**) Human VGLL3 FASTA sequence from Swissprot and used NetNES 1.1 (http://www.cbs.dtu.dk/services/NetNES/) to predict nuclear export signals (la Cour, T., Kiemer, L., Molgaard, A., Gupta, R., Skriver, K. and Brunak, S. (2004). Analysis and prediction of leucine-rich nuclear export signals. Protein Eng Des Sel 17, 527-36).
(**B**) Evolutionary conservation of the human, chimpanzee, cat and mouse Vgll3 protein sequences using Clustal Omega (https://www.ebi.ac.uk/Tools/msa/clustalo/).

Click here to Download Table S3

Table S4: Genes that are up- or down-regulated by 24 h or 48 h of Vgll3 expression in murine primary satellite cell-derived myoblasts
(A) Genes that are significantly 1.3-fold up or 1.3-fold down (indicated with a "-") regulated at 24 h.
(B) Genes that are significantly 1.3-fold up or 1.3-fold down (indicated with a "-") regulated at 48 h.
Gene expression analysis using Affymetrix Mouse Gene 2.0 ST microarrays. Vgll3 is mainly a repressor of gene expression (ratio 9 down versus 1 up at 24 h and 29 up versus 126 down at 48 h).
Key: Vgll2 regulated genes are other Tead1-4 binding proteins (Vgll2, Wwtr1), the Hippo negative feedback loop (Ajuba, Amotl2, Frmd6), the myogenic regulator factor Myf5, insulin-like growth factor-binding proteins (Igfbp2-4) and Wnt proteins (Wnt7b, Fzd4) as well as Pitx transcription factors (Pitx2, Pitx3). The effect on Hippo signalling proteins is typical for the effect of Hippo proteins on transcription, suggesting that Vgll3 partially regulates Hippo target genes.

Click here to Download Table S4

Table S5: Comparison of genes regulated by Vgll3 compared to Yap and Taz
Expression of either Vgll3, YAP1 S127A or TAZ S89A or empty vector for 24 h and 48 h in satellite cell-derived myoblasts. Gene expression analysis using Affymetrix Mouse Gene 2.0 ST microarrays. To avoid having to compare 6 datasets (Vgll3, Yap, Taz at 24 h and 48 h timepoints) we pooled the 24 h and 48 h time points. Vgll3 is mainly a repressor of gene expression and typically a Yap antagonist (examples: *Gzmd*, *Thbs1*) or co-represses genes with Yap (examples: *U90926*, *Trbj2-3*). In contrast, Vgll3 and Taz sometimes co-induce the same genes (examples: *Gzmd*, *Unc5c*).

Click here to Download Table S5

Table S6: Genes deregulated by Vgll3 overexpression in mouse are also deregulated in man VGLL3 was knocked down (via siRNA) or overexpressed (via retroviral transduction) in human myoblasts. Cells were analysed in proliferating conditions (myoblasts) or after 2 days in differentiation medium (myocytes). mRNA was extracted and expression of the genes affected by Vgll3 in mouse (Fig 3) were analysed by RT-qPCR. Gene expression was normalized to control sample (si Control or RV control respectively) and fold change compared to control. Most of the genes deregulated by Vgll3 overexpression in mouse were validated in human myoblasts. However, overexpression of VGLL3 in proliferative myoblasts induces WWTR1, represses EGFR1 and does not affect FRMD6, WNT7B, PITX2/3 or IGFBP2-3.Data are presented as fold change, where a red colour indicates a significant difference ($p < 0.05$) between test sample (knockdown or overexpression of VGLL3) and control using a paired two-tailed t-test, where n=3 independent experiments.

Click here to Download Table S6

Table S7: Vgll3 knockout does not affect fibre type distribution, fibre count, muscle weight, or cross-section area in hind limb muscles
(A) Total and relative fibre distribution in mouse soleus wildtype versus *Vgll3-/-* (mean values ± standard deviation).
(B) Cross-sectional area of muscle fibres in mouse soleus wildtype versus *Vgll3-/-* (mean values ± standard deviation).
(C) Absolute and relative weights of the hind limb muscles in relation to the total body weight.

Click here to Download Table S7

Table S8: Primary and secondary antibodies used

Antibody	Clone/Catalogue No.	Supplier	Concentration (IF)
Rabbit monoclonal anti-YAP	D8H1X	Cell Signaling	N/A
Mouse monoclonal anti-Myc	4A6	Merck	N/A
Mouse Monoclonal anti-Myogenin	F5D-s	DSHB	1/10
Mouse anti-MyHC	M20-c	DSHB	1/250
Mouse anti-β-Tubulin	E76-c	DSHB	1/300
Mouse anti-FLAG	F1804	Sigma	1/200
Chicken anti-GFP	ab13970	Abcam	1/2000
Rabbit anti-Laminin	L9393	Sigma	1/200
Mouse monoclonal anti MyHC1 Isotype IgG2b	BA.D5-c	DSHB	1/100
Mouse monoclonal anti-MyHC2a isotype IgG1	SC.71-c	DSHB	1/100
Mouse monoclonal anti-MyHC2b isotype IgM	BF.F3-c	DSHB	1/100
Secondary antibodies Alexa fluor 350 Goat anti-Mouse IgG2b, Alexa fluor 488 Goat anti-Mouse IgG1, Alexa fluor 594 Goat anti-Mouse IgG1 and Alexa fluor 488 or 633 Goat anti Rabbit		Invitrogen	1/500

Table S9: Primers used in the study

Gene	Forward primer (5'-3')	Reverse primer (5'-3')
Tbp	ATCCCAAGCGATTTGCTG	CCTGTGCACACCATTTTTCC
Vgll1	TTCAGGAGAACTGAAAGACGTG	GGGGGCATGCTCTTATTG
Vgll2	ACGCTTCCCAGCAAACAA	GGCTGGTCTTTCTCCTCCTC
Vgll3	GGATTCCTGCTCCCCAGT	TTGTCCTGATGCTGAAGACCT
Vgll4	TGTGAAAACGACCACGTCTC	GCAGTCTCCGTTGACAGTCTT
Pax7	CCGTGTTTCTCATGGTTGTG	GAGCACTCGGCTAATCGAAC
Myogenin	CTACAGGCCTTGCTCAGCTC	AGATTGTGGGCGTCTGTAGG
TBP	CGGCTGTTTAACTTCGCTTC	CACACGCCAAGAAACAGTGA
VGLL2	CTGTACCAGCAGCAAAGCAC	CATCGGGAAGGAGCAGTCT
VGLL3	TGGATGAACACTTCTCAAGAGC	GCTGGCTTGAGAGAGCTGAG
MYF5	CTATAGCCTGCCGGGACA	TGGACCAGACAGGACTGTTACAT
MYOGENIN	CCAGGGGTGCCCAGCGAATG	AGCCGTGAGCAGATGATCC
MyHC	AGCAGGAGGAGTACAAGAAG	CTTTGACCACCTTGGGCTTC
PITX2	CTGTGTGGACCAACCTTACG	CCGAAGCCATTCTTGCATA
PITX3	GAGTCTGCCTGTTGCAGGA	CAGCGTCTGACAGCGACA
WWTR1	ATTCGAATGCGCCAAGAG	AACTGGGGCAAGAGTCTCAG
AJUBA	TTTGTTTGCTGCTCTTGTGG	TGAAAACAGATAATCTTCCTCACAGT
AMOTL2	CAGCTTCAATGAGGGTCTGC	GCATGGAGCACCTTTAACCT
FRMD6	*CTGGTGCTCAAGACTTTCTCC*	*GGTTCCCAGCACTCCAAAG*
FSTL1	ACCCATCTTTCAACCCTCCT	GACACAGCGGTTACAGTCCA
EGFR	GTGGATGGCATTGGAATCA	CAAAGGTCATCAACTCCCAAA
WNT7B	TCATGAACCTGCATAACAATGAG	CCAGCAGGTTTTGGTGGT
FZD4	TTCACACCGCTCATCCAGTA	TGCACATTGGCACATAAACA
IGFBP2	CCAAGAAGCTGCGACCAC	GGGATGTGCAGGGAGTAGAG
IGFBP3	AACGCTAGTGCCGTCAGC	CGGTCTTCCTCCGACTCAC